

---

# Adaptive Sample-Efficient Blackbox Optimization via ES-active Subspaces

---

Krzysztof Choromanski<sup>\*1</sup> Aldo Pacchiano<sup>\*2</sup> Jack Parker-Holder<sup>\*3</sup> Yunhao Tang<sup>\*3</sup>

## Abstract

We present a new algorithm (ASEBO) for conducting optimization of high-dimensional blackbox functions. ASEBO adapts to the geometry of the function and learns optimal sets of sensing directions, which are used to probe it, on-the-fly. It addresses the exploration-exploitation trade-off of blackbox optimization, where each single function query is expensive, by continuously learning the bias of the lower-dimensional model used to approximate gradients of smoothings of the function with compressed sensing and contextual bandits methods. To obtain this model, it uses techniques from the emerging theory of active subspaces (Constantine, 2015) in the novel ES blackbox optimization context. As a result, ASEBO learns the dynamically changing intrinsic dimensionality of the gradient space and adapts to the hardness of different stages of the optimization without external supervision. Consequently, it leads to more sample-efficient blackbox optimization than state-of-the-art algorithms. We provide rigorous theoretical justification of the effectiveness of our method. We also empirically evaluate it on the set of reinforcement learning policy optimization tasks as well as functions from the recently open-sourced Nevergrad library (Teytaud & Rapin, 2018), demonstrating that it consistently learns optimal inputs with fewer queries to a blackbox function than other methods.

## 1. Introduction

Consider a high-dimensional function  $F : \mathbb{R}^d \rightarrow \mathbb{R}$ , where each function query is expensive. Examples include reinforcement learning (RL) blackbox functions taking as inputs vectors  $\theta$  encoding policies  $\pi : \mathcal{S} \rightarrow \mathcal{A}$  mapping states to actions and outputting total (expected/discounted) re-

wards obtained by agents applying  $\pi$  in given environments (Brockman et al., 2016). In this setting function evaluation usually requires a simulation used to score the performance of the particular policy. Other examples include wind configuration design optimization problems for high speed civil transport aircrafts, optimizing computer codes (e.g. NASA synthetic tool FLOPS/ENGGEN used to size the aircraft and propulsion system (Ahmad & Thomas, 2013)), crash tests/medical and chemical reaction experiments analysis and more (Zhou et al., 2017).

Evolution strategy (ES) methods have traditionally been used in low-dimensional regimes (e.g. hyperparameter tuning), and considered ill-equipped for higher dimensional problems due to poor sampling complexity (Nesterov & Spokoyny, 2017). However, a flurry of recent work has shown they can scale better than previously believed (Such et al., 2017; Conti et al., 2018; Rowland et al., 2018; Mania et al., 2018; Choromanski et al., 2018; Salimans et al., 2017; Liu et al., 2019). This is thanks to a couple of reasons.

First of all, new ES methods apply several efficient heuristics (filtering, various normalization techniques as in (Mania et al., 2018) and new exploration strategies as in (Conti et al., 2018)) in order to substantially improve sampling complexity. Other recent methods (Rowland et al., 2018; Choromanski et al., 2018) are based on more accurate Quasi Monte Carlo (MC) estimators of the gradients of Gaussian smoothings of blackbox functions with theoretical guarantees. These approaches provide better quality gradient sensing mechanisms, and also enable the practitioners to reduce the total number of conducted queries. Additionally, in applications such as RL, new compact structured policy architectures (such as low-displacement rank neural networks from (Choromanski et al., 2018) or even linear architectures as in (Rowland et al., 2018; Mania et al., 2018)) are used to reduce the number of parameters encoding policies and thus also the dimensionality of the optimization problem.

Recent research also shows ES-type blackbox optimization in RL leads to more stable policies than policy gradient methods by looking for parameters that are robust to perturbations (Lehman et al., 2018). This is true since unlike policy gradient methods, ES aims to find parameters maximizing expected reward over entire population of parameters rather than just a set of parameters maximizing the reward.

---

<sup>1</sup>Google Brain Robotics, New York, NY, USA <sup>2</sup>University of California Berkeley, Berkeley, CA, USA <sup>3</sup>Columbia University, NY, USA. Correspondence to: Krzysztof Choromanski <kchoro@google.com>.

Finally, pure ES methods have one clear advantage over state-of-the-art policy optimization techniques such as TRPO, PPO or ARS (Schulman et al., 2017; Hämmäläinen et al., 2018; Schulman et al., 2015; Mania et al., 2018). They can be applied for general blackbox optimization problems that do not necessarily exhibit the underlying MDP structure that is required for policy gradient methods and cannot benefit from state normalization algorithm central to ARS. This has led to their recent popularity for non-differentiable tasks (Houthoofd et al., 2018; Ha & Schmidhuber, 2018).

In this paper we introduce a new generic ES blackbox optimization algorithm (ASEBO), which adapts to the geometry of blackbox functions and learns optimal sets of sensing directions, which are used to probe the function, on-the-fly. To obtain this model, it uses techniques from the emerging theory of active subspaces (Constantine, 2015; Constantine et al., 2016; 2015) in a novel ES blackbox optimization context. It addresses the exploration-exploitation trade-off of blackbox optimization, where each single function query is expensive, by continuously learning the bias of the lower-dimensional model used to approximate gradients of smoothings of the function with compressed sensing and contextual bandits methods. The adaptiveness is what distinguishes it from some recently introduced guided ES methods such as (Maheswaranathan et al., 2018) that rely on hyperparameters that are hard to tune in advance, such as fixed (throughout entire algorithm) length of the buffer defining lower dimensional space for guided gradient search.

We provide rigorous theoretical justification of the effectiveness of ASEBO and empirically evaluate it on a set of reinforcement learning policy blackbox optimization tasks as well as non-RL blackbox functions from the recently open-sourced Nevergrad library (Teytaud & Rapin, 2018), showing that it consistently learns optimal inputs with fewer queries to a blackbox function than other methods.

The paper is organized as follows:

- In Section 2 we introduce the ASEBO algorithm and explain key theoretical ideas behind it, in particular we propose the notion of ES-active subspaces.
- In Section 3 we provide all theoretical results for the ASEBO algorithm.
- In Section 4 we conduct an empirical comparison of ASEBO with other blackbox optimization methods, in particular state-of-the-art RL algorithms designed for policy optimization.
- In the Appendix we present all the proofs, give additional experimental details and results.
- We provide final conclusions in Section 5.

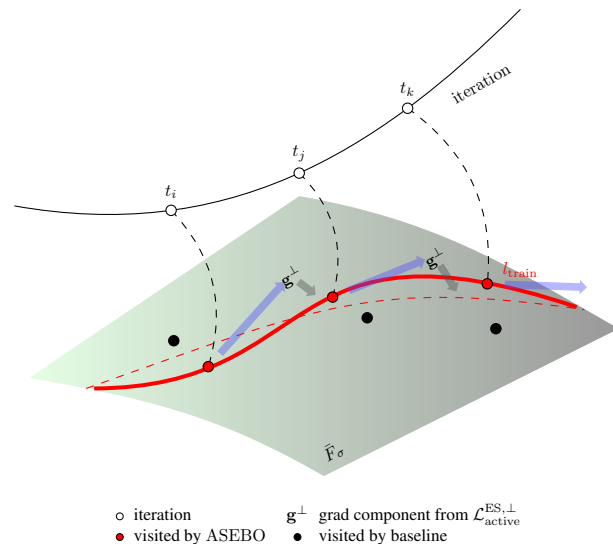


Figure 1. Pictorial representation of the ASEBO algorithm.  $\tilde{F}_\sigma$  stands for the denoised regularized version of  $F_\sigma$  that ASEBO exploits by keeping the PCA-driven active subspace  $\mathcal{L}_{\text{active}}^{\text{ES}}$  for gradient sensing and updating it on-the-fly. Blue arrows correspond to the components of the gradient-vectors from that subspace while grey ones to those  $\mathbf{g}^\perp$  from the orthogonal complement  $\mathcal{L}_{\text{active}}^{\text{ES},\perp}$ . The length of  $\mathbf{g}^\perp$  is constantly sensed via a much less expensive sub-procedure to determine how aggressively to do exploration. Black dots correspond to the baseline ES that does not take advantage of the local lower-dimensional representation of  $F_\sigma$ .

## 2. Adaptive Blackbox Optimization

Before we describe ASEBO, we explain key theoretical ideas behind the algorithm. ASEBO uses online PCA to maintain and update on-the-fly subspaces which we call *ES-active subspaces*  $\mathcal{L}_{\text{active}}^{\text{ES}}$ , accurately approximating the gradient data space at a given phase of the algorithm. The bias of the obtained gradient estimators is measured by sensing the length of its component from the orthogonal complement  $\mathcal{L}_{\text{active}}^{\text{ES},\perp}$  via compressed sensing or computing optimal probabilities for exploration (e.g. sensing from  $\mathcal{L}_{\text{active}}^{\text{ES},\perp}$ ) via contextual bandits methods (Agrawal et al., 2015). The algorithm corrects its probabilistic distributions used for choosing directions for gradient sensing based on these measurements. As we show, we can measure that bias accurately using only a constant number of additional function queries, regardless of the dimensionality. This in turn determines an exploration strategy, as we explain later. Estimated gradients are then used to update parameters and that completes a single iteration of the algorithm. ASEBO is presented schematically in Fig. 1.

### 2.1. Preliminaries

Consider a blackbox function  $F : \mathbb{R}^d \rightarrow \mathbb{R}$ . We do not assume that  $F$  is differentiable. The *Gaussian smoothing*

(Nesterov & Spokoiny, 2017)  $F_\sigma$  of  $F$  parameterized by smoothing parameter  $\sigma > 0$  is given as:

$$F_\sigma(\theta) = \mathbb{E}_{\mathbf{g} \in \mathcal{N}(0, \mathbf{I}_d)} [F(\theta + \sigma \mathbf{g})] = (2\pi)^{-\frac{d}{2}} \int_{\mathbb{R}^d} F(\theta + \sigma \mathbf{g}) e^{-\frac{\|\mathbf{g}\|^2}{2}} d\mathbf{g}. \quad (1)$$

The gradient of the Gaussian smoothing of  $F$  is given by the formula:

$$\nabla F_\sigma(\theta) = \frac{1}{\sigma} \mathbb{E}_{\mathbf{g} \sim \mathcal{N}(0, \mathbf{I}_d)} [F(\theta + \sigma \mathbf{g}) \mathbf{g}]. \quad (2)$$

Formula 2 on  $\nabla F_\sigma(\theta)$  leads straightforwardly to several unbiased Monte Carlo (MC) estimators of  $\nabla F_\sigma(\theta)$ , where the most popular ones are: the *forward finite difference* estimator (Choromanski et al., 2018) defined as:

$$\widehat{\nabla}_{\text{MC}}^{\text{FD}} F_\sigma(\theta) = \frac{1}{k\sigma} \sum_{i=1}^k (F(\theta + \sigma \mathbf{g}_i) - F(\theta)) \mathbf{g}_i, \quad (3)$$

and an *antithetic ES gradient estimator* (Salimans et al., 2017) given as:

$$\widehat{\nabla}_{\text{MC}}^{\text{AT}} F_\sigma(\theta) = \frac{1}{2k\sigma} \sum_{i=1}^k (F(\theta + \sigma \mathbf{g}_i) - F(\theta - \sigma \mathbf{g}_i)) \mathbf{g}_i, \quad (4)$$

where typically  $\mathbf{g}_1, \dots, \mathbf{g}_k$  are taken independently at random from  $\mathcal{N}(0, \mathbf{I}_d)$ . Samples  $\mathbf{g}_1, \dots, \mathbf{g}_k$  can be also  $L_2$ -normalized Gaussian vectors (not necessarily independent) or taken from more complex joint distributions. We call samples  $\mathbf{g}_1, \dots, \mathbf{g}_k$  the *sensing directions* since they are used to sense gradients  $\nabla F_\sigma(\theta)$ . If they are  $L_2$ -normalized and further, conditioned to be orthogonal as in recently proposed structured MC estimators of gradients of Gaussian smoothings (Choromanski et al., 2018) and if  $F$  is smooth, then Formula 4 can be alternatively rationalized as giving the renormalized gradient of  $F$ , if not taking into account cubic and higher-order terms of the Taylor expansion  $F(\theta + \mathbf{v}) = F(\theta) + \nabla F^\top \mathbf{v} + \frac{1}{2} \mathbf{v}^\top H(\theta) \mathbf{v}$  (where  $H(\theta)$  stands for the Hessian of  $F$  in  $\theta$ ).

Standard ES methods apply different gradient-based techniques such as SGD or Adam, fed with the above MC estimators of  $\nabla F_\sigma$  to conduct blackbox optimization. The number of samples  $k$  per iteration of the optimization procedure is usually of the order  $O(d)$ . This becomes a computational bottleneck for high-dimensional blackbox functions  $F$  (for instance, even for relatively small RL tasks with policies encoded by compact neural networks we still have  $d > 100$  parameters).

## 2.2. ES-active subspaces via online PCA with decaying weights

The first idea leading to the ASEBO algorithm is that in practice one does not need to estimate the gradient

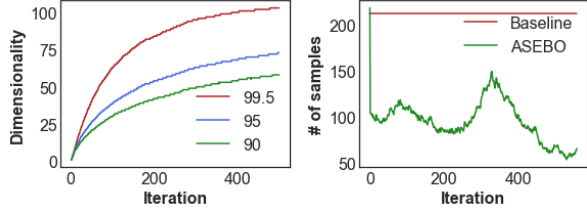


Figure 2. The motivation behind the ASEBO algorithm. On the left: ES baseline for the HalfCheetah task from the OpenAI Gym library for 212-dimensional policies - the plot shows how the dimensionality of the space capturing a given percentage of variance of approximate gradient data depends on the iteration of the algorithm. This information is never exploited by the algorithm, even though 99.5% of the variance resides in the much lower-dimensional space (100 dimensions). On the right: The ASEBO algorithm taking advantage of this information. The number of samples (sensing directions) reflects the hardness of the optimization at each iteration and is strongly correlated with the PCA dimensionality.

of  $F$  accurately (after all ES-type methods do not even aim to compute the gradient of  $F$ , but rather focus on  $\nabla F_\sigma$ ). Poor scalability of the ES-type blackbox optimization algorithms is caused by high-dimensionality of the gradient vector. However, during the optimization process the space spanned by gradients may be locally well approximated by a lower-dimensional subspace  $\mathcal{L}$  and sensing the gradient in that subspace might be more effective. In some recent papers such as (Maheswaranathan et al., 2018) such a subspace is defined simply as  $\mathcal{L} = \text{span}\{\widehat{\nabla}_{\text{MC}}^{\text{AT}} F_\sigma(\theta_i), \widehat{\nabla}_{\text{MC}}^{\text{AT}} F_\sigma(\theta_{i-1}), \dots, \widehat{\nabla}_{\text{MC}}^{\text{AT}} F_\sigma(\theta_{i-s+1})\}$ , where  $\{\widehat{\nabla}_{\text{MC}}^{\text{AT}} F_\sigma(\theta_i), \widehat{\nabla}_{\text{MC}}^{\text{AT}} F_\sigma(\theta_{i-1}), \dots, \widehat{\nabla}_{\text{MC}}^{\text{AT}} F_\sigma(\theta_{i-s+1})\}$  stands for the batch of last  $s$  approximated gradients during the optimization process and  $s$  is a fixed hyperparameter.

Even though  $\mathcal{L}$  will dynamically change during the optimization, such an approach has several disadvantages in practice. Tuning parameter  $s$  is very difficult or almost impossible and the assumption that the dimensionality of  $\mathcal{L}$  should be constant during optimization is usually false. In our approach the dimensionality of  $\mathcal{L}$  varies depending on the hardness of the optimization in different optimization stages.

We apply Principal Component Analysis (PCA, (Jolliffe, 2002)) to create a subspace  $\mathcal{L}$  capturing particular variance  $\sigma > 0$  of the approximate gradients data. Choosing  $\sigma$  (see Section 4) is in practice much easier than choosing  $s$  and leads to subspaces  $\mathcal{L}$  of varying dimensionalities throughout the optimization procedure, called by us from now on *ES-active subspaces*  $\mathcal{L}_{\text{active}}^{\text{ES}}$ . These will be in turn applied to define covariance matrices encoding multivariate probabilistic distributions applied to construct sensing directions used for estimating  $\nabla F_\sigma(\theta)$ . We will present two methods

for constructing these covariance matrices (see: Subsection 2.4 for details). The additional advantage of our approach is that PCA automatically filters out gradient noise.

---

**Algorithm 1** ASEBO Algorithm

**Hyperparameters:** number of iterations of full sampling  $l$ , smoothing parameter  $\sigma > 0$ , step size  $\eta$ , PCA threshold  $\epsilon$ , decay rate  $\gamma$ , total number of iterations  $T$ .

**Input:** blackbox function  $F$ , vector  $\theta_0 \in \mathbb{R}^d$  where optimization starts.  $\text{Cov}_0 \in \{0\}^{d \times d}$ ,  $p^0 = 0$ .

**Output:** vector  $\theta_T$ .

**for**  $t = 0, \dots, T - 1$  **do**

**if**  $t < l$  **then**

    Take  $n_t = d$ . Sample  $\mathbf{g}_1, \dots, \mathbf{g}_{n_t}$  from  $\mathcal{N}(0, \mathbf{I}_d)$  (independently).

**else**

    1. Take top  $r$  eigenvalues  $\lambda_i$  of  $\text{Cov}_t$ , where  $r$  is smallest such that:  $\sum_{i=1}^r \lambda_i \geq \epsilon \sum_{i=1}^d \lambda_i$ , using its SVD as described in text and take  $n_t = r$ .

    2. Take the corresponding eigenvectors  $\mathbf{u}_1, \dots, \mathbf{u}_r \in \mathbb{R}^d$  and denote by  $\mathbf{U} \in \mathbb{R}^{d \times r}$  a matrix obtained by stacking them together. Denote by  $\mathbf{U}^{\text{act}} \in \mathbb{R}^{d \times r}$  a matrix obtained from stacking together some orthonormal basis of  $\mathcal{L}_{\text{active}}^{\text{ES}} \stackrel{\text{def}}{=} \text{span}\{\mathbf{u}_1, \dots, \mathbf{u}_r\}$ . Denote by  $\mathbf{U}^\perp \in \mathbb{R}^{d \times (d-r)}$  a matrix obtained from stacking together some orthonormal basis of the orthogonal complement  $\mathcal{L}_{\text{active}}^{\text{ES}, \perp}$  of  $\mathcal{L}_{\text{active}}^{\text{ES}}$ .

    3. Sample  $\mathbf{g}_1, \dots, \mathbf{g}_{n_t}$  from  $\mathcal{N}(0, \sigma \Sigma)$  (independently), where  $\Sigma = \frac{1-p^t}{d} \mathbf{I}_d + \frac{p^t}{r} \mathbf{U} \mathbf{U}^\top (\mathbf{V1})$  or sample  $n_t$  vectors  $\mathbf{g}_1, \dots, \mathbf{g}_{n_t}$  as follows: with probability  $1-p^t$  from  $\mathcal{N}(0, \mathbf{U}^\perp (\mathbf{U}^\perp)^\top)$  and with probability  $p^t$  from  $\mathcal{N}(0, \mathbf{U}^{\text{act}} (\mathbf{U}^{\text{act}})^\top)$  (**V2**).

    4. Renormalize  $\mathbf{g}_1, \dots, \mathbf{g}_{n_t}$  such that marginal distributions  $\|\mathbf{g}_i\|_2$  are  $\chi(d)$ .

1. Compute  $\widehat{\nabla}_{\text{MC}}^{\text{AT}} F(\theta_t)$  as:

$$\widehat{\nabla}_{\text{MC}}^{\text{AT}} F(\theta_t) = \frac{1}{2n_t \sigma} \sum_{j=1}^{n_t} (F(\theta_t + \mathbf{g}_j) - F(\theta_t - \mathbf{g}_j)) \mathbf{g}_j$$

2. Set  $\text{Cov}_{t+1} = \lambda \text{Cov}_t + (1 - \lambda) \Gamma$ , where  $\Gamma = \widehat{\nabla}_{\text{MC}}^{\text{AT}} F_\sigma(\theta_t) (\widehat{\nabla}_{\text{MC}}^{\text{AT}} F_\sigma(\theta_t))^\top$

3. Set  $p^{t+1} = p_{\text{opt}}$  for  $p_{\text{opt}}$  output by Algorithm 3 or  $p^{t+1} = \frac{\widehat{r}}{\widehat{r}+1}$ , where:

$$\widehat{r} = \frac{\|(\widehat{\nabla} F_\sigma(\theta_t))_{\text{active}}\|_2}{\|(\widehat{\nabla} F_\sigma(\theta_t))_\perp\|_2},$$

is computed by Algorithm 2 and scalars  $\|(\widehat{\nabla} F_\sigma(\theta_t))_{\text{active}}\|_2$ ,  $\|(\widehat{\nabla} F_\sigma(\theta_t))_\perp\|_2$  stand for the estimates of  $\|(\nabla F_\sigma(\theta_t))_{\text{active}}\|_2$  and  $\|(\nabla F_\sigma(\theta_t))_\perp\|_2$ .

4. Set  $\theta_{t+1} \leftarrow \theta_t + \eta \widehat{\nabla}_{\text{MC}}^{\text{AT}} F(\theta_t)$ .

---

We use our own online version of PCA with decaying weights (decay rate is defined by parameter  $\lambda > 0$ ). By tuning  $\lambda$  we can define the rate at which historical approximate gradient data is used to choose the right sensing directions, which will continuously decay.

---

**Algorithm 2** Explore estimator via compressed sensing

**Hyperparameters:** smoothing parameter  $\sigma$ , horizon  $C$ .

**Input:** subspaces:  $\mathcal{L}_{\text{active}}^{\text{ES}}$ ,  $\mathcal{L}_{\text{active}}^{\text{ES}, \perp}$ , function  $F$ , vector  $\theta_t$ .

**Output:** ratio  $\widehat{r}$ .

1. Initialize square norm averages  $s_0^{\text{active}} = s_0^\perp = 0$ .

**for**  $l = 1, \dots, C$  **do**

  1. Sample  $\mathbf{g}_l^{\text{active}} \sim \mathcal{N}(0, \sigma \mathbf{I}_{\mathcal{L}_{\text{active}}^{\text{ES}}})$ .

  2. Sample  $\mathbf{g}_l^\perp \sim \mathcal{N}(0, \sigma \mathbf{I}_{\mathcal{L}_{\text{active}}^{\text{ES}, \perp}})$ .

  3. Ask for  $F(\theta_t \pm \mathbf{g}_l^{\text{type}})$  for type  $\in \{\text{active}, \perp\}$ .

  4. Compute  $v_l^{\text{type}} = \frac{1}{2\sigma} (F(\theta_t + \mathbf{g}_l^{\text{type}}) - F(\theta_t - \mathbf{g}_l^{\text{type}}))$ .

  5. Compute  $s_l^{\text{active}} = \frac{l-1}{l} * s_{l-1}^{\text{active}} + \frac{(v_l^{\text{active}})^2}{l}$ .

  6. Compute  $s_l^\perp = \frac{l-1}{l} * s_{l-1}^\perp + \frac{(v_l^\perp)^2}{l}$ .

**Return:**  $\widehat{r} = \sqrt{\frac{s_C^{\text{active}}}{s_C^\perp}}$ .

---



---

**Algorithm 3** Explore estimator via exponentiated sampling

**Hyperparameters:** smoothing parameter  $\sigma$ , horizon  $C$ , learning rate  $\alpha$ , probability regularizer  $\beta$ .

**Input:** subspaces:  $\mathcal{L}_{\text{active}}^{\text{ES}}$ ,  $\mathcal{L}_{\text{active}}^{\text{ES}, \perp}$ , function  $F$ , vector  $\theta_t$ , initial probability parameter  $q_0^t \in (0, 1)$ .

**Output:**

**for**  $l = 1, \dots, C + 1$  **do**

  1. Compute  $p_{l-1}^t = (1 - 2\beta)q_{l-1}^t + \beta$

  2. Sample  $a_l^t \sim \text{Ber}(p_l^t)$ .

  3. If  $a_l^t = 1$ , sample  $\mathbf{g}_l \sim \mathcal{N}(0, \sigma \mathbf{I}_{\mathcal{L}_{\text{active}}^{\text{ES}}})$ , otherwise sample  $\mathbf{g}_l \sim \mathcal{N}(0, \sigma \mathbf{I}_{\mathcal{L}_{\text{active}}^{\text{ES}, \perp}})$ .

  4. Compute  $v_l = \frac{1}{2\sigma} (F(\theta_t + \mathbf{g}_l) - F(\theta_t - \mathbf{g}_l))$ .

  5. Set  $\mathbf{e}_l = (1 - 2\beta) \begin{bmatrix} -\frac{a_l^t (\dim(\mathcal{L}_{\text{active}}^{\text{ES}}) + 2)}{(p_l^t)^3} \\ -\frac{(1-a_l^t) (\dim(\mathcal{L}_{\text{active}}^{\text{ES}, \perp}) + 2)}{(1-p_l^t)^3} \end{bmatrix} v_l^2$ .

  6.  $q_l^t = \frac{q_{l-1}^t \exp(-\alpha \mathbf{e}_l(1))}{q_{l-1}^t \exp(-\alpha \mathbf{e}_l(1)) + (1-q_{l-1}^t) \exp(-\alpha \mathbf{e}_l(2))}$ .

**Return:**  $p_C$ .

---

We consider a stream of approximate gradients  $\widehat{\nabla}_{\text{MC}}^{\text{AT}} F_\sigma(\theta_0), \dots, \widehat{\nabla}_{\text{MC}}^{\text{AT}} F_\sigma(\theta_i), \dots$  obtained during the optimization procedure. We maintain and update on-the-fly the covariance matrix  $\text{Cov}_t$ , where  $t$  stands for the number of completed iterations, in the form of the symmetric matrix SVD-decomposition  $\text{Cov}_t = \mathbf{Q}_t^\top \Sigma_t \mathbf{Q}_t \in \mathbb{R}^d$ . When the new approximate gradient  $\widehat{\nabla}_{\text{MC}}^{\text{AT}} F_\sigma(\theta_t)$  arrives, the update of the covariance matrix is driven by the following equation, reflecting data decay process:

$$\mathbf{Q}_{t+1}^\top \Sigma_{t+1} \mathbf{Q}_{t+1} = \lambda \mathbf{Q}_t^\top \Sigma_t \mathbf{Q}_t + (1 - \lambda) \mathbf{x}_t \mathbf{x}_t^\top, \quad (5)$$

where  $\mathbf{x}_t = \widehat{\nabla}_{\text{MC}}^{\text{AT}} F_\sigma(\theta_t)$ .

To conduct the update cheaply, it suffices to observe that the RHS of Equation 5 can be rewritten as:  $\lambda \mathbf{Q}_t^\top \Sigma_t \mathbf{Q}_t + (1-\lambda) \mathbf{x}_t \mathbf{x}_t^\top = \mathbf{Q}_t^\top (\lambda \Sigma_t + (1-\lambda) \mathbf{Q}_t \mathbf{x}_t (\mathbf{Q}_t \mathbf{x}_t)^\top) \mathbf{Q}_t$ . Now, using the fact that for a matrix of the form  $\mathbf{D} + \mathbf{u}\mathbf{u}^\top$ , we can get its decomposition in time  $O(d^2)$  (Golub, 1973), we obtain an algorithm performing updates in quadratic time. That in practice suffices since the bottleneck of the computations is in blackbox function evaluations and the additional overhead related to updating  $\mathcal{L}_{\text{active}}^{\text{ES}}$  subspace is negligible (see: Section 4 for details).

**ES-active subspaces versus active subspaces:** Our mechanism for constructing  $\mathcal{L}_{\text{active}}^{\text{ES}}$  is inspired by the recent theory of active subspaces (Constantine, 2015) which is being developed to determine the most important directions in the space of input parameters of high-dimensional blackbox functions such as computer simulations. The *active subspace* of a differentiable function  $F : \mathbb{R}^d \rightarrow \mathbb{R}$ , square-integrable with respect to the given probabilistic density function  $\rho : \mathbb{R}^d \rightarrow \mathbb{R}$ , is given as a linear subspace  $\mathcal{L}_{\text{active}}$  defined by the first  $r$  (for a fixed  $r < d$ ) eigenvectors of the following  $d \times d$  symmetric positive definite matrix:

$$\text{Cov} = \int_{\mathbf{x} \in \mathbb{R}^d} \nabla F(\mathbf{x}) \nabla F(\mathbf{x})^\top \rho(\mathbf{x}) d\mathbf{x} \quad (6)$$

Here density function  $\rho$  determines regions, where lower-dimensional representation of  $F$  is needed. In our approach we do not assume differentiability of  $F$ , but the key difference between  $\mathcal{L}_{\text{active}}^{\text{ES}}$  and  $\mathcal{L}_{\text{active}}$  lies somewhere else. The goal of ASEBO is to avoid approximating the exact gradient  $\nabla F(\mathbf{x}) \in \mathbb{R}^d$  which is what makes standard ES methods very expensive and which is done in (Constantine et al., 2015) via gradient sketching techniques combined with finite difference approaches (standard methods of choice for ES baselines). Instead, in ASEBO an ES-active subspace  $\mathcal{L}_{\text{active}}^{\text{ES}}$  is itself used to define sensing directions and the number of chosen samples  $k$  is given by the dimensionality of  $\mathcal{L}_{\text{active}}^{\text{ES}}$ . This drastically reduces sampling complexity, but comes at a price of risking the optimization to be trapped permanently in the fixed lower-dimensional space that will not be representative for gradient data as the optimization progresses. We address this crucial problem and propose a solution requiring only a constant number of extra queries to function  $F$  in the next sections.

### 2.3. Exploration-exploitation trade-off: Adaptive Exploration Mechanism

The procedure described above needs to be accompanied with an exploration strategy that will determine how frequently to choose sensing directions outside the constructed on-the-fly lower-dimensional ES-subspace  $\mathcal{L}_{\text{active}}^{\text{ES}}$ . Our exploration strategies will be encoded by hybrid probabilistic

distributions for sampling sensing directions. The frequency of sensing from the distributions with covariance matrices obtained from  $\mathcal{L}_{\text{active}}^{\text{ES}}$  (corresponding to exploitation) and from its orthogonal complement  $\mathcal{L}_{\text{active}}^{\text{ES},\perp}$  or entire space (corresponding to exploration) will be given by weights encoding the importance of exploitation versus exploration in any given iteration of the optimization. For a vector  $\mathbf{x} \in \mathbb{R}^d$  denote by  $\mathbf{x}_{\text{active}}$  its projection onto  $\mathcal{L}_{\text{active}}^{\text{ES}}$  and by  $\mathbf{x}_\perp$  its projection onto  $\mathcal{L}_{\text{active}}^{\text{ES},\perp}$ . The metric that ASEBO uses to update the above weights in an online manner in the  $t^{\text{th}}$  iteration of the algorithm is the ratio:

$$r = \frac{\|(\nabla F_\sigma(\theta_t))_{\text{active}}\|_2}{\|(\nabla F_\sigma(\theta_t))_\perp\|_2}. \quad (7)$$

Smaller values of  $r$  indicate that current active subspace is not representative enough for the gradient and more aggressive exploration needs to be conducted. In practice, we do not compute  $r$  explicitly, but rather its approximated version  $\widehat{r}$ . One can simply take:  $\widehat{r} = \frac{\|(\widehat{\nabla}_{\text{MC}}^{\text{AT}} F_\sigma(\theta_{t-1}))_{\text{active}}\|_2}{\|(\widehat{\nabla}_{\text{MC}}^{\text{AT}} F_\sigma(\theta_{t-1}))_\perp\|_2}$ , where  $\widehat{\nabla}_{\text{MC}}^{\text{AT}} F_\sigma(\theta_{t-1})$  stands for the vector obtained in the previous iteration. However we can do better. Observe first that it suffices to separately estimate  $\|(\nabla F_\sigma(\theta_t))_{\text{active}}\|_2$  and  $\|(\nabla F_\sigma(\theta_t))_\perp\|_2$ . However we do not aim to estimate  $(\nabla F_\sigma(\theta_t))_{\text{active}}$  and  $(\nabla F_\sigma(\theta_t))_\perp$ . That would be equivalent to computing exact estimate of  $\nabla F_\sigma(\theta_t)$ , defeating the purpose of ASEBO. Instead, we use the observation that estimating the length of the unknown high-dimensional vector is much simpler than estimating the vector itself and can be done in the probabilistic manner with arbitrary precision via the set of dot-product queries of size independent from dimensionality  $d$ . We propose compressed sensing techniques to do it (see: Algorithm 2 box for details). By refining that approach, we come up with a more accurate contextual bandits method that also relies on dot-product queries applied in the ES-context, but this time aims to directly approximate optimal probabilities of sampling from  $\mathcal{L}_{\text{active}}^{\text{ES}}$  rather than approximating gradients components' lengths (see Algorithm 3 box). For both methods the related computational overhead is measured in constant number of extra blackbox function queries, negligible in practice.

### 2.4. The Algorithm

We are ready to present the ASEBO algorithm in detail. The main procedure is given in the Algorithm 1 box. The algorithms we apply to score the relative importance of sampling from the ES-active subspace  $\mathcal{L}_{\text{active}}^{\text{ES}}$  versus from outside  $\mathcal{L}_{\text{active}}^{\text{ES}}$  are given in the Algorithm 2 box and the Algorithm 3 box. Algorithm 2 is using compressed sensing methods to determine the lengths of the components of the gradient from subspaces  $\mathcal{L}_{\text{active}}^{\text{ES}}$  and  $\mathcal{L}_{\text{active}}^{\text{ES},\perp}$  to calculate  $\widehat{r}$ . Algorithm 3 instead uses a bandits method to determine optimal probability of sampling from  $\mathcal{L}_{\text{active}}^{\text{ES}}$ ,

without explicitly approximating these components. In the next section we show that by using these techniques we can substantially reduce the variance of ES blackbox gradient estimators if ES-active subspaces approximate the gradient data well (which is the case for RL blackbox functions as presented in Fig. 2). Horizon lengths  $C$  in Algorithms: 2 and 3 which determines the number of extra function queries should be in practice chosen as small constants. In each iteration of Algorithm 1 the number of function queries is proportional to the dimensionality of the ES-active subspace  $\mathcal{L}_{\text{active}}^{\text{ES}}$  rather than the original space and this is where we obtain substantial computational gains.

### 3. Theoretical Results

In this section we provide theoretical guarantees for the ASEBO sampling mechanism, where sensing directions  $\{\mathbf{g}_i\}$  at time  $t$  are sampled from the distribution used in version **V2** of Algorithm 1:

$$\hat{P} = \begin{cases} \mathbf{g} \sim \mathcal{N}(0, \mathbf{I}_{\mathcal{L}_{\text{active}}^{\text{ES}}}) & \text{with probability } p^t \\ \mathbf{g} \sim \mathcal{N}(0, \mathbf{I}_{\mathcal{L}_{\text{active}}^{\perp}}) & \text{with probability } 1 - p^t, \end{cases}$$

where  $p^t$  is a probability parameter with values in  $[0, 1]$ .

Following notation in Algorithm 1, denote by  $\mathbf{U}^{\text{act}} \in \mathbb{R}^{d \times r}$  a matrix obtained by stacking together vectors of some orthonormal basis of  $\mathcal{L}_{\text{active}}^{\text{ES}}$ , where  $\dim(\mathcal{L}_{\text{active}}^{\text{ES}}) = r$  and by  $\mathbf{U}^{\perp} \in \mathbb{R}^{d \times (d-r)}$  a matrix obtained from stacking together vectors of some orthonormal basis of its orthogonal complement  $\mathcal{L}_{\text{active}}^{\text{ES}, \perp}$ . Denote by  $\sigma$  a smoothing parameter.

We make the following regularity assumptions on  $F$ :

**Assumption 1.**  $F$  is  $L$ -Lipschitz, i.e. for all  $\theta, \theta' \in \mathbb{R}^d$ ,  $|F(\theta) - F(\theta')| \leq L\|\theta - \theta'\|_2$  for some  $L > 0$ .

**Assumption 2.**  $F$  has a  $\tau$ -smooth third order derivative tensor with respect to  $\sigma > 0$ , so that  $F(\theta + \sigma \mathbf{g}) = F(\theta) + \sigma \nabla F(\theta)^\top \mathbf{g} + \frac{\sigma^2}{2} \mathbf{g}^\top H(\theta) \mathbf{g} + \frac{1}{6} \sigma^3 F'''(\theta)[\mathbf{v}, \mathbf{v}, \mathbf{v}]$  for some  $\mathbf{v} \in \mathbb{R}^d$  ( $\|\mathbf{v}\|_2 \leq \|\mathbf{g}\|_2$ ) satisfying  $|F'''(\theta)[\mathbf{v}, \mathbf{v}, \mathbf{v}]| \leq \tau \|\mathbf{v}\|_2^3 \leq \tau \|\mathbf{g}\|_2^3$ .

Under these assumptions, the one-sample baseline antithetic estimator  $\widehat{\nabla}_{\text{MC}, k=1}^{\text{AT, base}} F_\sigma(\theta)$  of  $\nabla F_\sigma(\theta)$  given as:  $\widehat{\nabla}_{\text{MC}, k=1}^{\text{AT, base}} F_\sigma(\theta) := \frac{F(\theta + \sigma \mathbf{g}) \mathbf{g} + F(\theta + \sigma \mathbf{g})(-\mathbf{g})}{2\sigma}$  for  $\mathbf{g} \sim \mathcal{N}(0, \mathbf{I}_d)$  satisfies  $\widehat{\nabla}_{\text{MC}, k=1}^{\text{AT, base}} F_\sigma(\theta) = \mathbf{g} \mathbf{g}^\top \nabla F(\theta) + \xi_{\mathbf{g}}(\theta) \mathbf{g}$  such that  $|\xi_{\mathbf{g}}(\theta)| \leq \tau \sigma^2 \|\mathbf{g}\|_2^3$ . An analogous statement is true for the corresponding ASEBO one-sample estimator corresponding to sensings sampled from  $\hat{P}$ . Observe also that the following is true:

$$\mathbb{E}_{\mathbf{g} \sim \hat{P}} [\mathbf{g} \mathbf{g}^\top] = \underbrace{\left( p^t \mathbf{U}^{\text{act}} (\mathbf{U}^{\text{act}})^\top + (1 - p^t) \mathbf{U}^{\perp} (\mathbf{U}^{\perp})^\top \right)}_{\mathbf{C}_1}$$

Let  $\widehat{\nabla}_{\text{MC}, k=1}^{\text{AT, asebo}} F_\sigma(\theta) = \mathbf{C}_1^{-1} \frac{F(\theta + \sigma \mathbf{g}) \mathbf{g} + F(\theta + \sigma \mathbf{g})(-\mathbf{g})}{2\sigma}$  be the gradient estimator corresponding to  $\hat{P}$  (we tested empirically that the inverse covariance renormalization factor  $\mathbf{C}_1^{-1}$  does not change learning profiles in practice, but we incorporate it here since it is needed for rigorous theoretical analysis). We start by showing that under the assumption of noiseless evaluation of  $F$ , both the bias of  $\widehat{\nabla}_{\text{MC}, k=1}^{\text{AT, base}} F_\sigma(\theta)$  and the bias of  $\widehat{\nabla}_{\text{MC}, k=1}^{\text{AT, asebo}} F_\sigma(\theta)$  are small. Let  $\epsilon > 0$ . Throughout this section we will assume that  $\sigma$  is small enough, i.e.  $\sigma < \frac{1}{35} \sqrt{\frac{\epsilon \min(p^t, 1 - p^t)}{\tau d^3 \max(L, 1)}}$  for some precision parameter  $\epsilon > 0$ .

**Lemma 3.1.** *If  $F$  satisfies Assumptions 1 and 2, the gradient estimators  $\widehat{\nabla}_{\text{MC}, k=1}^{\text{AT, base}} F_\sigma(\theta)$  and  $\widehat{\nabla}_{\text{MC}, k=1}^{\text{AT, asebo}} F_\sigma(\theta)$  satisfy:*

$$\begin{aligned} \left\| \mathbb{E}_{\mathbf{g} \sim \mathcal{N}(0, \mathbf{I}_d)} \left[ \widehat{\nabla}_{\text{MC}, k=1}^{\text{AT, base}} F_\sigma(\theta) \right] - \nabla F(\theta) \right\| &\leq \epsilon \\ \left\| \mathbb{E}_{\mathbf{g} \sim \hat{P}} \left[ \widehat{\nabla}_{\text{MC}, k=1}^{\text{AT, asebo}} F_\sigma(\theta) \right] - \nabla F(\theta) \right\| &\leq \epsilon \end{aligned}$$

Consequently  $\mathbb{E}_{\mathbf{g} \sim \mathcal{N}(0, \mathbf{I}_d)} \left[ \mathbf{U}^{\text{act}} (\mathbf{U}^{\text{act}})^\top \widehat{\nabla}_{\text{MC}, k=1}^{\text{AT, base}} F_\sigma(\theta) \right] \approx (\nabla F(\theta_t))_{\text{active}}$  and  $\mathbb{E}_{\mathbf{g} \sim \hat{P}} \left[ \mathbf{U}^{\text{act}} (\mathbf{U}^{\text{act}})^\top \widehat{\nabla}_{\text{MC}, k=1}^{\text{AT, asebo}} F_\sigma(\theta) \right] \approx (\nabla F(\theta_t))_{\text{active}}$  and analogous statements hold for  $\mathbf{U}^{\perp}$ .

#### 3.1. Estimating ratio $r$ for “exploring how to explore”

In this section we provide guarantees for the estimation of the ratio  $r$  as specified in Equation 7 for Algorithm 2.

Let  $s_{\mathbf{U}^{\text{act}}} = \|(\mathbf{U}^{\text{act}})^\top \nabla F(\theta)\|_2^2$  and  $s_{\mathbf{U}^{\perp}} = \|(\mathbf{U}^{\perp})^\top \nabla F(\theta)\|_2^2$ . The results of this section hinge on the observation that whenever  $\mathbf{g} \sim \mathcal{N}(0, \mathbf{I}_{\mathcal{L}_{\text{active}}^{\text{ES}}})$  the distribution of  $\frac{F(\theta + \sigma \mathbf{g}) - F(\theta - \sigma \mathbf{g})}{2\sigma} \approx N(0, s_{\mathbf{U}^{\text{act}}})$ . Analogously when  $\mathbf{g} \sim \mathcal{N}(0, \mathbf{I}_{\mathcal{L}_{\text{active}}^{\text{ES}, \perp}})$  the distribution of  $\frac{F(\theta_t + \sigma \mathbf{g}) - F(\theta_t - \sigma \mathbf{g})}{2\sigma} \approx N(0, s_{\mathbf{U}^{\perp}})$ . The next theorem quantifies how large horizon  $C$  from both theorems should be to obtain a good empirical approximation for the ratio  $r$ .

**Theorem 3.2.** *Let  $0 < s < C$  and let  $\mathbf{g}_i \sim \mathcal{N}(0, \mathbf{I}_{\mathcal{L}_{\text{active}}^{\text{ES}}})$  for  $i = 1, \dots, s$  and  $\mathbf{g}_i \sim \mathcal{N}(0, \mathbf{I}_{\mathcal{L}_{\text{active}}^{\text{ES}, \perp}})$  for  $i = s + 1, \dots, C$ .*

*Let  $\hat{s}_{\mathbf{U}^{\text{act}}} := \frac{1}{s} \sum_{j=1}^s \left( \frac{F(\theta + \sigma \mathbf{g}_j) - F(\theta - \sigma \mathbf{g}_j)}{2\sigma} \right)^2$ ,  $\hat{s}_{\mathbf{U}^{\perp}} := \frac{1}{C-s} \sum_{j=1}^{C-s} \left( \frac{F(\theta + \sigma \mathbf{g}_j) - F(\theta - \sigma \mathbf{g}_j)}{2\sigma} \right)^2$  and let  $\hat{r} = \sqrt{\frac{\hat{s}_{\mathbf{U}^{\text{act}}}}{\hat{s}_{\mathbf{U}^{\perp}}}}$ . Given  $u, \epsilon > 0$  and  $\delta \in (\epsilon, 1)$ , the following holds.*

1. *If  $C = 2s$  for  $s \geq \frac{16}{u^2} \log\left(\frac{8}{\delta}\right)$  and under the mechanism from Algorithm 2 or*
2. *If  $\{\mathbf{g}_i\}_{i=1}^C$  are samples generated under  $\hat{P}$ ,  $\min(p^t, 1 - p^t) > u$  and  $C \geq \max\left(\frac{8}{(p^t - u)u^2}, \frac{8}{(1 - p^t - u)u^2}, \frac{2p^t + 2u/3}{u^2}\right) \log\left(\frac{12}{\delta}\right)$ ,*

then with probability at least  $1 - \delta$ :

$$\sqrt{\frac{s_{\mathbf{U}^{\text{act}}}(1-u) - \frac{2\epsilon}{\delta}}{s_{\mathbf{U}^\perp}(1+u) + \frac{2\epsilon}{\delta}}} \leq \hat{r} \leq \sqrt{\frac{s_V(1+u) + \frac{2\epsilon}{\delta}}{s_{V^\perp}(1-u) - \frac{2\epsilon}{\delta}}}.$$

### 3.2. Variance reduction via non isotropic sampling

We show now that under the sampling strategy encoded by distribution  $\hat{P}$ , the variance of the gradient estimator can be made smaller by choosing the probability parameter  $p^t$  appropriately. We conclude that given an appropriate subspace partition  $\mathcal{L}_{\text{active}}^{\text{ES}}, \mathcal{L}_{\text{active}}^{\text{ES},\perp}$  and the right choice of  $p^t$ , the variance of  $\hat{\nabla}_{\text{MC},k=1}^{\text{AT,asebo}} F_\sigma(\theta)$  can be orders of magnitude smaller than the variance of  $\hat{\nabla}_{\text{MC},k=1}^{\text{AT,base}} F_\sigma(\theta)$ . Denote:  $d_{\text{active}} = \dim(\mathcal{L}_{\text{active}}^{\text{ES}})$  and  $d_\perp = \dim(\mathcal{L}_{\text{active}}^{\text{ES},\perp})$ . The following holds:

**Lemma 3.3.** *The variance of  $\hat{\nabla}_{\text{MC},k=1}^{\text{AT,asebo}} F_\sigma(\theta)$  satisfies:*

$$|\text{Var}[\hat{\nabla}_{\text{MC},k=1}^{\text{AT,asebo}} F_\sigma(\theta)] - \Gamma| \leq \epsilon$$

for  $\Gamma = \frac{d_{\text{active}}+2}{p^t} s_{\mathbf{U}^{\text{act}}} - \frac{d_\perp+2}{1-p^t} s_{\mathbf{U}^\perp} + \|\nabla F(\theta)\|^2$ .

The choice of  $p^t$  that minimizes  $\Gamma$  equals:

$$p_*^t = \frac{\sqrt{(s_{\mathbf{U}^{\text{act}}})(d_{\text{active}} + 2)}}{\sqrt{(s_{\mathbf{U}^{\text{act}}})(d_{\text{active}} + 2) + \sqrt{(s_{\mathbf{U}^\perp})(d_\perp + 2)}}}.$$

**Lemma 3.4.** *The optimal variance  $\text{Var}_{\text{opt}}$  corresponding to  $p_*^t$  satisfies:  $|\text{Var}_{\text{opt}} - \Delta| \leq \epsilon$  for  $\Delta = \left[ \sqrt{(s_{\mathbf{U}^{\text{act}}})(d_{\text{active}} + 2) + \sqrt{(s_{\mathbf{U}^\perp})(d_\perp + 2)}} \right]^2 - \|\nabla F(\theta)\|^2$ .*

Our main theoretical result in this subsection states that:

**Theorem 3.5.**  $\text{Var}_{\text{opt}} \leq \text{Var}[\hat{\nabla}_{\text{MC},k=1}^{\text{AT,base}} F_\sigma(\theta)] + \epsilon - \lambda$  where

$$\lambda := \left| \sqrt{(s_{\mathbf{U}^\perp})(d_{\text{active}} + 2) + \sqrt{(s_{\mathbf{U}^{\text{act}}})(d_\perp + 2)}} - \sqrt{(s_{\mathbf{U}^{\text{act}}})(d_\perp + 2)} \right|^2 - 2\|\nabla F(\theta)\|^2.$$

*The slack  $\lambda$  is always nonnegative. The inequality is strict, for example when  $s_{\mathbf{U}^\perp} = 0$  and  $d_\perp \geq 1$ . In this case  $\text{Var}[\hat{\nabla}_{\text{MC},k=1}^{\text{AT,base}} F_\sigma(\theta)] \approx (d+1)\|\nabla F(\theta)\|^2$  whereas  $\text{Var}_{\text{opt}} \approx (d_{\text{active}} + 1)\|\nabla F(\theta)\|^2$ . Thus achieved gains can be substantial.*

### 3.3. Adaptive Mirror Descent

In Theorem 3.5 we proved that for appropriate choices of  $\mathcal{L}_{\text{active}}^{\text{ES}}$  and  $p_t$ , gradient estimator  $\hat{\nabla}_{\text{MC},k=1}^{\text{AT,asebo}} F_\sigma(\theta)$  will have significantly smaller variance than  $\hat{\nabla}_{\text{MC},k=1}^{\text{AT,base}} F_\sigma(\theta)$ . In this section we show that Algorithm 3 provides an adaptive way to choose  $p^t$ . Using tools from contextual bandits theory,

we provide regret guarantees that quantify the rate at which this Algorithm 3 minimizes the variance of  $\hat{\nabla}_{\text{MC},k=1}^{\text{AT,asebo}} F_\sigma(\theta)$  and converges to the optimal  $p_*^t$ .

Let  $\mathbf{p}_l^t = \begin{pmatrix} p_l^t \\ 1-p_l^t \end{pmatrix}$ . The main component  $\Gamma$  of the variance of  $\hat{\nabla}_{\text{MC},k=1}^{\text{AT,asebo}} F_\sigma(\theta)$  as a function of  $\mathbf{p}_l^t$  equals (Lemma 3.3) :

$$\Gamma = \ell(\mathbf{p}_l^t) = \frac{d_{\text{active}} + 2}{\mathbf{p}_l^t(1)} s_{\mathbf{U}^{\text{act}}} + \frac{d_\perp + 2}{\mathbf{p}_l^t(2)} s_{\mathbf{U}^\perp} - \|\nabla F(\theta)\|^2.$$

The gradient  $\nabla_{\mathbf{p}_l^t} \ell(\mathbf{p}_l^t)$  satisfies:

$$\nabla_{\mathbf{p}_l^t} \ell(\mathbf{p}_l^t) = \begin{pmatrix} -\frac{d_{\text{active}}+2}{(\mathbf{p}_l^t(1))^2} s_{\mathbf{U}^{\text{act}}} \\ -\frac{d_\perp+2}{(\mathbf{p}_l^t(2))^2} s_{\mathbf{U}^\perp} \end{pmatrix} = \mathbb{E} \left[ \begin{pmatrix} -\frac{a_l^t(d_{\text{active}}+2)}{(\mathbf{p}_l^t(1))^3} \\ -\frac{(1-a_l^t)(d_\perp+2)}{(\mathbf{p}_l^t(2))^2} \end{pmatrix} v_l^2 \right],$$

where  $a_l^t, v_l$  are defined as in Algorithm 3.

**Theorem 3.6.** *If  $F$  satisfies Assumptions 1 and 2,  $\sigma < \frac{1}{35} \sqrt{\frac{\epsilon \min(p^t, 1-p^t)}{\tau d^3 \max(L, 1)}}$ ,  $\alpha = \frac{2\beta^2}{\sqrt{C} \sqrt{(d_{\text{active}}+2)^2 s_{\mathbf{U}^{\text{act}}} + (d_\perp+2) s_{\mathbf{U}^\perp}}}$*

*and  $\epsilon = \frac{\beta^3}{2C(d+1)}$  then Algorithm 3 satisfies:*

$$\frac{1}{C} \mathbb{E} \left[ \sum_{l=1}^C \ell(\mathbf{p}_l^t) \right] - \min_{\mathbf{p} \in \beta + (1-2\beta)\Delta_2} \ell(\mathbf{p}) \leq \frac{\text{Var}_{\text{opt}}}{\beta^2 \sqrt{C}} + \frac{1}{C}$$

Where  $\Delta_2$  denotes the two dimensional simplex.

## 4. Experiments

We used different classes of high-dimensional blackbox functions to compare ASEBO with state-of-the-art methods. The first consisted of RL blackbox functions, where the input is a high-dimensional vector encoding a neural network policy  $\pi : \mathcal{S} \rightarrow \mathcal{A}$  mapping states  $s$  to actions  $a$  and the output is the (noisy) cumulative rewards obtained by an agent applying this policy in a particular environment. The second class consists of functions from the recently open-sourced Nevergrad library (Teytaud & Rapin, 2018), containing high-dimensional blackbox functions and generic blackbox optimization algorithms for benchmarking.

### 4.1. RL blackbox functions

We used the following environments from the OpenAI Gym library: Swimmer-v2, HalfCheetah-v2, Walker2d-v2, Reacher-v2, Hopper-v2 and Linear Quadratic Regulator (LQR) environment from (Mania et al., 2018) (results for the latter two are presented in the Appendix). Aside from LQR, all blackbox RL functions have  $> 100$  input parameters. For this class of blackbox functions we compared ASEBO with other generic blackbox methods as well as those specializing in optimizing RL blackbox functions  $F$  (e.g. PPO/TRPO) by taking advantage of the MDP structure of  $F$  that ASEBO is agnostic to. Tested gradient-based algorithms use the Adam optimizer for parameter updates.

In all experiments we used policies encoded by low-displacement rank neural network architectures with Toeplitz matrices from (Choromanski et al., 2018) of two hidden layers and with tanh nonlinearities. We compared ASEBO (ours) with the following algorithms:

- Covariance Matrix Adaptation Evolution Strategy algorithm (CMA-ES; we used its pycma open-source implementation from <https://github.com/CMA-ES/pycma>),
- Vanilla ES algorithm (standard evolution strategy random-search based optimization from (Salimans et al., 2017) without virtual batch norm since considered compressed policies have fewer parameters)
- Augmented Random Search (ARS) (Mania et al., 2018) (we used implementation released by the authors at <http://github.com/modestyachts/ARS>)
- Proximal Policy Optimization (PPO) (Schulman et al., 2017) and Trust Region Policy Optimization (TRPO) (Schulman et al., 2015) (we used OpenAI baseline implementation (Dhariwal et al., 2017))

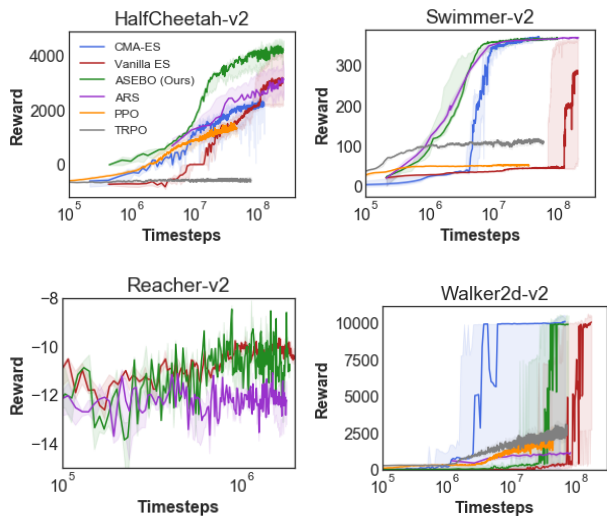


Figure 3. Comparison of different blackbox optimization algorithms on OpenAI Gym tasks. All curves are median-curves obtained from  $k = 10$  seeds and with inter-quartile ranges presented as shadowed regions. PPO, TRPO and CMA-ES curves are not presented on Reacher-v2 subfigure since these algorithms did not learn in a given timeframe, we present the full plots that include all algorithms in Appendix 7. Best policies learned here by ASEBO manage to solve the task successfully.

For each algorithm we used  $k = 10$  seeds and obtained curves are median-curves with inter-quartile ranges presented as shadowed regions. The results of four environments are presented on Fig. 3 and we show the rest in

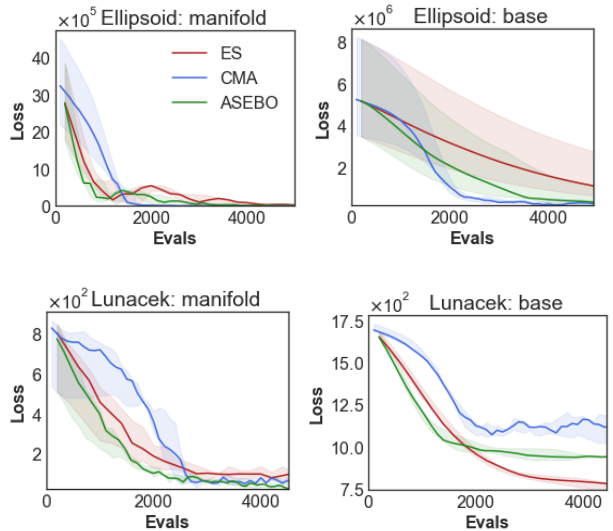


Figure 4. Comparison of different blackbox optimization algorithms on functions from Nevergrad library (Teytaud & Rapin, 2018). All curves are median-curves obtained from  $k = 5$  seeds and with inter-quartile ranges presented as shadowed regions.

Appendix 7. Sample complexity is measured in the number of timesteps (environment transitions) used by the algorithms (notice the log scale). ASEBO is the only algorithm that is in top-2 for all six environments, outperforming baseline ES-type methods on all of them and being the best on Swimmer-v2, HalfCheetah-v2 and Reacher-v2.

#### 4.2. Nevergrad blackbox functions

We tested functions: cigar, ellipsoid, sphere, sphere4 and lunacek (from the class of Bi-Rastrigin/Lunacek’s No.02 functions) from the Nevergrad library (Teytaud & Rapin, 2018). We created two versions of each function  $F$ : base, where the function directly depends on the higher-dimensional input and manifold: where it implicitly depends on the manifold of lower intrinsic dimensionality  $d_{int}$ . In the latter one the manifold and  $d_{int}$  are not known in advance. This time we used  $k = 5$  seeds and as before, show median curves. The results are presented on Fig. 4 (see: Appendix for additional results). Even though CMA-ES outperforms ASEBO for base versions, when  $F$  admits a structure (manifold version), ASEBO beats other methods.

### 5. Conclusion

We proposed a new algorithm for optimizing high-dimensional blackbox functions. ASEBO adjusts on-the-fly the strategy of choosing gradient sensing directions to the hardness of the problem at the current stage of optimization and can be applied for both RL and non-RL problems.

## References

- Agrawal, S., Devanur, N. R., and Li, L. Contextual bandits with global constraints and objective. *CoRR*, abs/1506.03374, 2015. URL <http://arxiv.org/abs/1506.03374>.
- Ahmad, S. and Thomas, K. B. Flight optimization system ( fops ) hybrid electric aircraft design capability. 2013.
- Brockman, G., Cheung, V., Pettersson, L., Schneider, J., Schulman, J., Tang, J., and Zaremba, W. OpenAI Gym, 2016.
- Choromanski, K., Rowland, M., Sindhvani, V., Turner, R. E., and Weller, A. Structured evolution with compact architectures for scalable policy optimization. In *Proceedings of the 35th International Conference on Machine Learning, ICML 2018, Stockholm, Sweden, July 10-15, 2018*, pp. 969–977, 2018. URL <http://proceedings.mlr.press/v80/choromanski18a.html>.
- Constantine, P. G. *Active Subspaces - Emerging Ideas for Dimension Reduction in Parameter Studies*, volume 2 of *SIAM spotlights*. SIAM, 2015. ISBN 978-1-611-97385-3. URL <http://bookstore.siam.org/s102/>.
- Constantine, P. G., Eftekhari, A., and Wakin, M. B. Computing active subspaces efficiently with gradient sketching. In *6th IEEE International Workshop on Computational Advances in Multi-Sensor Adaptive Processing, CAMSAP 2015, Cancun, Mexico, December 13-16, 2015*, pp. 353–356, 2015. doi: 10.1109/CAMSAP.2015.7383809. URL <https://doi.org/10.1109/CAMSAP.2015.7383809>.
- Constantine, P. G., Kent, C., and Bui-Thanh, T. Accelerating markov chain monte carlo with active subspaces. *SIAM J. Scientific Computing*, 38(5), 2016. doi: 10.1137/15M1042127. URL <https://doi.org/10.1137/15M1042127>.
- Conti, E., Madhavan, V., Such, F. P., Lehman, J., Stanley, K. O., and Clune, J. Improving exploration in evolution strategies for deep reinforcement learning via a population of novelty-seeking agents. In *Advances in Neural Information Processing Systems 31: Annual Conference on Neural Information Processing Systems 2018, NeurIPS 2018, 3-8 December 2018, Montréal, Canada.*, pp. 5032–5043, 2018.
- Dhariwal, P., Hesse, C., Klimov, O., Nichol, A., Plappert, M., Radford, A., Schulman, J., Sidor, S., Wu, Y., and Zhokhov, P. Openai baselines. <https://github.com/openai/baselines>, 2017.
- Duan, Y., Chen, X., Houthoofd, R., Schulman, J., and Abbeel, P. Benchmarking deep reinforcement learning for continuous control. In *International Conference on Machine Learning*, pp. 1329–1338, 2016.
- Golub, G. H. Some modified matrix eigenvalue problems. *SIAM*, 15, 1973.
- Ha, D. and Schmidhuber, J. Recurrent world models facilitate policy evolution. *NeurIPS*, 2018.
- Hämäläinen, P., Babadi, A., Ma, X., and Lehtinen, J. Ppocma: Proximal policy optimization with covariance matrix adaptation. *CoRR*, abs/1810.02541, 2018.
- Hansen, N. and Ostermeier, A. Adapting arbitrary normal mutation distributions in evolution strategies: The covariance matrix adaptation. In *Evolutionary Computation, 1996., Proceedings of IEEE International Conference on*, pp. 312–317. IEEE, 1996.
- Houthoofd, R., Chen, Y., Isola, P., Stadie, B., Wolski, F., Jonathan Ho, O., and Abbeel, P. Evolved policy gradients. *NeurIPS*, 2018.
- Jolliffe, I. Principal component analysis. *Series: Springer Series in Statistics*, XXIX, 2002.
- Lehman, J., Chen, J., Clune, J., and Stanley, K. O. ES is more than just a traditional finite-difference approximator. In *Proceedings of the Genetic and Evolutionary Computation Conference, GECCO 2018, Kyoto, Japan, July 15-19, 2018*, pp. 450–457, 2018. doi: 10.1145/3205455.3205474. URL <https://doi.org/10.1145/3205455.3205474>.
- Liu, G., Zhao, L., Yang, F., Bian, J., Qin, T., Yu, N., and Liu, T.-Y. Trust region evolution strategies. In *AAAI*, 2019.
- Maheswaranathan, N., Metz, L., Tucker, G., and Sohl-Dickstein, J. Guided evolutionary strategies: escaping the curse of dimensionality in random search. *CoRR*, abs/1806.10230, 2018. URL <http://arxiv.org/abs/1806.10230>.
- Mania, H., Guy, A., and Recht, B. Simple random search provides a competitive approach to reinforcement learning. *CoRR*, abs/1803.07055, 2018. URL <http://arxiv.org/abs/1803.07055>.
- Nesterov, Y. and Spokoiny, V. Random gradient-free minimization of convex functions. *Found. Comput. Math.*, 17(2):527–566, April 2017. ISSN 1615-3375.
- Rowland, M., Choromanski, K., Chalus, F., Pacchiano, A., Sarlos, T., Turner, R. E., and Weller, A. Geometrically coupled monte carlo sampling. In *NeurIPS*, 2018.

Salimans, T., Ho, J., Chen, X., Sidor, S., and Sutskever, I. Evolution strategies as a scalable alternative to reinforcement learning. 2017.

Schulman, J., Levine, S., Abbeel, P., Jordan, M. I., and Moritz, P. Trust region policy optimization. In *Proceedings of the 32nd International Conference on Machine Learning, ICML 2015, Lille, France, 6-11 July 2015*, pp. 1889–1897, 2015. URL <http://jmlr.org/proceedings/papers/v37/schulman15.html>.

Schulman, J., Wolski, F., Dhariwal, P., Radford, A., and Klimov, O. Proximal policy optimization algorithms. *arXiv preprint arXiv:1707.06347*, 2017.

Such, F. P., Madhavan, V., Conti, E., Lehman, J., Stanley, K. O., and Clune, J. Deep neuroevolution: Genetic algorithms are a competitive alternative for training deep neural networks for reinforcement learning. *CoRR*, abs/1712.06567, 2017. URL <http://arxiv.org/abs/1712.06567>.

Teytaud, O. and Rapin, J. Nevergrad: An open source tool for derivative-free optimization. <https://code.fb.com/ai-research/nevergrad/>, 2018.

Zhou, Z., Li, X., and Zare, R. N. Optimizing chemical reactions with deep reinforcement learning. *ACS Central Science*, 3(12):1337–1344, 2017. doi: 10.1021/acscentsci.7b00492. URL <https://doi.org/10.1021/acscentsci.7b00492>. PMID: 29296675.

## APPENDIX: Adaptive Sample-Efficient Blackbox Optimization via Active Subspaces

### 6. Theoretical Results

Throughout this section we will assume the sensings directions  $\{\mathbf{g}_i\}$  at time  $t$  are sampled from one of the following families of distributions:

$$\widehat{P} = \begin{cases} \mathbf{g} \sim \mathcal{N}(0, \mathbf{I}_{\mathcal{L}_{\text{active}}^{\text{ES}}}) & \text{with probability } p^t \\ \mathbf{g} \sim \mathcal{N}(0, \mathbf{I}_{\mathcal{L}_{\text{active}}^{\text{ES}, \perp}}) & \text{with probability } 1 - p^t \end{cases}$$

Where  $p^t$  is a probability parameter with values in  $[0, 1]$ .

Denote an by  $\mathbf{U}^{\text{ort}} \in \mathbb{R}^{d \times d_{\text{active}}}$  an orthonormal basis of the active subspace  $\mathcal{L}_{\text{active}}^{\text{ES}}$  and  $\mathbf{U}^{\perp} \in \mathbb{R}^{d \times d - d_{\text{active}}}$  an orthonormal basis of  $\mathcal{L}_{\text{active}}^{\text{ES}, \perp}$ .

Let's start by computing the covariance matrix of  $\widehat{P}$ :

$$\mathbb{E}_{\mathbf{g} \sim P_t} [\mathbf{g}\mathbf{g}^{\top}] = \underbrace{(p^t \mathbf{U}^{\text{ort}} (\mathbf{U}^{\text{ort}})^{\top} + (1 - p^t) \mathbf{U}^{\perp} (\mathbf{U}^{\perp})^{\top})}_{\mathbf{C}_1}$$

In order to simplify the notation of the proofs in this section we use the following conventions:

$$\begin{aligned} z_{ES} &= \widehat{\nabla}_{\text{MC}, k=1}^{\text{AT}, \text{base}} F_{\sigma}(\theta) \\ z_1 &= \widehat{\nabla}_{\text{MC}, k=1}^{\text{AT}, \text{asebo}} F_{\sigma}(\theta) \end{aligned}$$

Where  $z_1$  is the ASEBO gradient estimator resulting form using sampling mechanism  $\widehat{P}$ .

To simplify notation we also use  $\mathbf{U}$  instead of  $\mathbf{U}^{\text{ort}}$ ,  $\mathbf{I}_{\mathbf{U}}$  instead of  $\mathbf{I}_{\mathcal{L}_{\text{active}}^{\text{ES}}}$  and  $\mathbf{I}_{\mathbf{U}^{\perp}}$  instead of  $\mathbf{I}_{\mathcal{L}_{\text{active}}^{\text{ES}, \perp}}$ .

Let  $\epsilon > 0$  be the precision parameter. We choose  $\sigma$  with the goal of making the bias between the expectation of our gradient estimators and the true gradient of  $F$  smaller than  $\epsilon$ . Throughout this section we assume  $\sigma$  is small enough:

$$0 < \sigma < \frac{1}{35} \sqrt{\frac{\epsilon \min(p^t, 1 - p^t)}{\tau d^3 \max(L, 1)}}$$

#### 6.1. Gradient Estimators, their bias and their variance.

We make the following assumptions on  $F$ :

**Assumption 1.**  $F$  is  $L$ -Lipschitz. For all  $\theta, \theta' \in \mathbb{R}^d$ ,  $|F(\theta) - F(\theta')| \leq L \|\theta - \theta'\|$ .

**Assumption 2.**  $F$  has a  $\tau$ -smooth third order derivative tensor, so that  $F(\theta + \sigma \mathbf{g}) = F(\theta) + \sigma \nabla F(\theta)^{\top} \mathbf{g} + \frac{\sigma^2}{2} \mathbf{g}^{\top} H(\theta) \mathbf{g} + \frac{1}{6} \sigma^3 F'''(\theta)[v, v, v]$  with  $v \in [0, \mathbf{g}]$  satisfying  $|F'''(\theta)[v, v, v]| \leq \tau \|v\|^3 \leq \tau \|\mathbf{g}\|^3$ .

Let  $d_{\text{active}}$  and  $d_{\perp}$  denote the dimensionality of  $\mathcal{L}_{(\text{active})}$  and  $\mathcal{L}_{\perp}$  respectively.

Under these assumptions,  $\frac{F(\theta_t + \sigma \mathbf{g}) - F(\theta_t - \sigma \mathbf{g})}{2\sigma} = (\mathbf{g}^{\top} \nabla F(\theta_t)) + \xi_{\mathbf{g}}(\theta_t)$  such that  $\xi_{\mathbf{g}}(\theta_t) \leq \frac{\tau}{6} \sigma^2 \|\mathbf{g}\|^3$ , uniformly over all  $\theta_t$ . We relax the constants slightly. If  $F$ 's third order derivative tensor is smooth with constant  $\tau$ :

$$\left| \frac{F(\theta_t + \sigma \mathbf{g}) - F(\theta_t - \sigma \mathbf{g})}{2\sigma} - \mathbf{g}^{\top} \nabla F(\theta_t) \right| \leq \tau \sigma^2 \|\mathbf{g}\|^3.$$

Recall the following definitions:

- **Evolution Strategies Gradient.** Let  $\mathbf{g} \sim \mathcal{N}(0, \mathbf{I})$ . The ES gradient is defined as  $z_{ES} = \frac{F(\theta_t + \sigma \mathbf{g}) - F(\theta_t - \sigma \mathbf{g})}{2\sigma} \mathbf{g}$ .
- **$\hat{P}$  Nonisotropic Gradient.** Let  $\mathbf{g} \sim \hat{P}$ . The  $\hat{P}$  gradient is defined as  $z_1 = \mathbf{C}_1^{-1} \frac{F(\theta_t + \sigma \mathbf{g}) - F(\theta_t - \sigma \mathbf{g})}{2\sigma} \mathbf{g}$ .

The following inequalities hold:

$$\begin{aligned} \|\xi_{\mathbf{g}}(\theta_t) \mathbf{g}\|^2 &\leq \frac{\tau}{6} \sigma^2 \|\mathbf{g}\|^4 \\ \|\mathbb{E}_{\mathbf{g} \sim \mathcal{N}(0, \mathbf{I})} [\xi_{\mathbf{g}}(\theta_t) \mathbf{g}]\|^2 &\leq \frac{\sigma^4 \tau^2}{36} (\mathbb{E}_{\mathbf{g} \sim \mathcal{N}(0, \mathbf{I})} [\|\mathbf{g}\|^4])^2 \leq \frac{\sigma^4 \tau^2 d^4}{4} \\ \|\mathbb{E}_{\mathbf{g} \sim \mathcal{N}(0, \mathbf{I}_{\mathbf{U}})} [\xi_{\mathbf{g}}(\theta_t) \mathbf{g}]\|^2 &\leq \frac{\sigma^4 \tau^2}{36} (\mathbb{E}_{\mathbf{g} \sim \mathcal{N}(0, \mathbf{I}_{\mathbf{U}^\perp})} [\|\mathbf{g}\|^4])^2 \leq \frac{\sigma^4 \tau^2 d_{\text{active}}^4}{4} \\ \|\mathbb{E}_{\mathbf{g} \sim \mathcal{N}(0, \mathbf{I}_{\mathbf{U}})} [\xi_{\mathbf{g}}(\theta_t) \mathbf{g}]\|^2 &\leq \frac{\sigma^4 \tau^2}{36} (\mathbb{E}_{\mathbf{g} \sim \mathcal{N}(0, \mathbf{I}_{\mathbf{U}^\perp})} [\|\mathbf{g}\|^4])^2 \leq \frac{\sigma^4 \tau^2 d_{\perp}^4}{4} \end{aligned}$$

### Bounding the Bias

**Theorem 6.1.** *The evolution strategies gradient estimator  $z_{ES}$  satisfies:*

$$\|\mathbb{E}_{\mathbf{g} \sim \mathcal{N}(0, \mathbf{I})} [z_{ES}] - \nabla F(\theta_t)\| \leq 3\tau\sigma^2 d^2 \quad (8)$$

$$\text{If } \sigma < \frac{1}{35} \sqrt{\frac{\epsilon \min(p^t, 1-p^t)}{\tau d^3 \max(L, 1)}}:$$

$$\|\mathbb{E}_{\mathbf{g} \sim \mathcal{N}(0, \mathbf{I})} [z_{ES}] - \nabla F(\theta_t)\| \leq \epsilon \quad (9)$$

*Proof.* Notice that  $\|\mathbf{g}\|^4 = (\sum_{i=1}^d \mathbf{g}(i)^2)^2 \leq d \sum_{i=1}^d \mathbf{g}(i)^4$ . Where we denote  $\mathbf{g}(i)$  as the  $i$ -th entry of the  $d$ -dimensional vector  $\mathbf{g} \in \mathbb{R}^d$ . Since  $\mathbb{E}[\mathbf{g}(i)^4] = 3$  for all  $i$ :

$$\mathbb{E}_{\mathbf{g} \sim \mathcal{N}(0, \mathbf{I})} [\|\mathbf{g}\|^4] \leq 3d^2$$

And therefore:

$$\left\| \mathbb{E}_{\mathbf{g} \sim \mathcal{N}(0, \mathbf{I})} \left[ \frac{F(\theta_t + \sigma \mathbf{g}) - F(\theta_t - \sigma \mathbf{g})}{2\sigma} \mathbf{g} \right] - \nabla F(\theta_t) \right\| \leq \tau\sigma^2 \mathbb{E}_{\mathbf{g} \sim \mathcal{N}(0, \mathbf{I})} [\|\mathbf{g}\|^4] \leq 3\tau\sigma^2 d^2$$

□

A similar result holds for the  $z_1$  gradient.

**Theorem 6.2.** *The non isotropic  $\hat{P}$  gradient estimator satisfies:*

$$\|\mathbb{E}_{\mathbf{g} \sim \hat{P}} [z_1] - \nabla F(\theta_t)\| \leq \frac{3\sigma^2 \tau}{p^t} d_{\text{active}}^2 + \frac{3\sigma^2 \tau}{1-p^t} d_{\perp}^2$$

$$\text{If } \sigma < \frac{1}{35} \sqrt{\frac{\epsilon \min(p^t, 1-p^t)}{\tau d^3 \max(L, 1)}}:$$

$$\|\mathbb{E}_{\mathbf{g} \sim \hat{P}} [z_1] - \nabla F(\theta_t)\| \leq \epsilon$$

*Proof.* Expanding  $\mathbb{E}_{\mathbf{g} \sim \hat{P}} [z_1]$  yields:

$$\begin{aligned} \mathbb{E}_{\mathbf{g} \sim \hat{P}} [z_1] &= \mathbf{C}_1^{-1} \mathbb{E}_{\mathbf{g} \sim \hat{P}} \left[ \frac{F(\theta_t + \sigma \mathbf{g}) - F(\theta_t - \sigma \mathbf{g})}{2\sigma} \mathbf{g} \right] \\ &= \mathbf{C}_1^{-1} \mathbb{E}_{\mathbf{g} \sim \hat{P}} [\mathbf{g} \mathbf{g}^\top \nabla F(\theta_t) + \xi_{\mathbf{g}}(\theta_t) \mathbf{g}] \\ &= \nabla F(\theta_t) + \frac{1}{p^t} \mathbb{E}_{\mathbf{g} \sim \mathcal{N}(0, \mathbf{I}_{\mathbf{U}})} [\xi_{\mathbf{g}}(\theta_t) \mathbf{g}] + \frac{1}{1-p^t} \mathbb{E}_{\mathbf{g} \sim \mathcal{N}(0, \mathbf{I}_{\mathbf{U}^\perp})} [\xi_{\mathbf{g}}(\theta_t) \mathbf{g}] \end{aligned}$$

By a similar argument as in the proof of Theorem 6.1:

$$\begin{aligned}\|\mathbb{E}_{\mathbf{g} \sim \mathcal{N}(0, \mathbf{I}_U)} [\xi_{\mathbf{g}}(\theta_t) \mathbf{g}]\| &\leq 3\tau\sigma^2 d_{\text{active}}^2 \\ \|\mathbb{E}_{\mathbf{g} \sim \mathcal{N}(0, \mathbf{I}_{U^\perp})} [\xi_{\mathbf{g}}(\theta_t) \mathbf{g}]\| &\leq 3\tau\sigma^2 d_\perp^2\end{aligned}$$

The result follows.  $\square$

In fact, the distance between the square norms of the expectation of the ES gradient and the true gradient of  $F$  are also bounded:

**Theorem 6.3.** *If  $F$  satisfies Assumption 1 and 2:*

$$\left| \|\mathbb{E}_{\mathbf{g} \sim \mathcal{N}(0, \mathbf{I})} [z_{ES}]\|^2 - \|\nabla F(\theta_t)\|^2 \right| \leq 105\tau^2\sigma^4 d^4 + 6\tau\sigma^2 L d^2 \quad (10)$$

$$\text{If } \sigma < \frac{1}{35} \sqrt{\frac{\epsilon \min(p^t, 1-p^t)}{\tau d^3 \max(L, 1)}}.$$

$$\left| \|\mathbb{E}_{\mathbf{g} \sim \mathcal{N}(0, \mathbf{I})} [z_{ES}]\|^2 - \|\nabla F(\theta_t)\|^2 \right| \leq \epsilon \quad (11)$$

*Proof.*

$$\begin{aligned}\left| \left\| \mathbb{E}_{\mathbf{g} \sim \mathcal{N}(0, \mathbf{I})} \left[ \frac{F(\theta_t + \sigma \mathbf{g}) - F(\theta_t - \sigma \mathbf{g})}{2\sigma} \mathbf{g} \right] \right\|^2 - \|\nabla F(\theta_t)\|^2 \right| &\leq \tau^2 (\sigma^2 \mathbb{E}_{\mathbf{g} \sim \mathcal{N}(0, \mathbf{I})} [\|\mathbf{g}\|^4])^2 + 2\tau\sigma^2 \|\nabla F(\theta_t)\| \|\mathbb{E}_{\mathbf{g} \sim \mathcal{N}(0, \mathbf{I})} [\|\mathbf{g}\|^4]\| \\ &\leq 105\tau^2\sigma^4 d^4 + 6\tau\sigma^2 L d^2\end{aligned}$$

$\square$

**Theorem 6.4.** *If  $F$  satisfies Assumption 1 and 2:*

$$\left| \|\mathbb{E}_{\mathbf{g} \sim \hat{\mathcal{P}}} [z_1]\|^2 - \|\nabla F(\theta_t)\|^2 \right| \leq \frac{1}{(p^t)^2} \frac{\sigma^4 \tau^2 d_{\text{active}}^4}{4} + \frac{1}{(1-p^t)^2} \frac{\sigma^4 \tau^2 d_\perp^4}{4} + \frac{2}{p^t} L \frac{\sigma^2 \tau d_{\text{active}}^2}{4} + \frac{2}{1-p^t} L \frac{\sigma^2 \tau d_\perp^2}{4} + \frac{2}{p^t(1-p^t)} \frac{\sigma^4 \tau^2 d_{\text{active}}^2 d_\perp^2}{16}$$

$$\text{If } \sigma < \frac{1}{35} \sqrt{\frac{\epsilon \min(p^t, 1-p^t)}{\tau d^3 \max(L, 1)}}.$$

$$\left| \|\mathbb{E}_{\mathbf{g} \sim \hat{\mathcal{P}}} [z_1]\|^2 - \|\nabla F(\theta_t)\|^2 \right| \leq \epsilon$$

*Proof.* Consider the following expansion of  $\mathbb{E}[z_1]$ .

$$\begin{aligned}\|\mathbb{E}_{\mathbf{g} \sim \hat{\mathcal{P}}} [z_1]\|^2 &= \|\nabla F(\theta_t)\|^2 + \frac{1}{(p^t)^2} \|\mathbb{E}_{\mathbf{g} \sim \mathcal{N}(0, \mathbf{I}_U)} [\xi_{\mathbf{g}}(\theta_t) \mathbf{g}]\|^2 + \left( \frac{1}{1-p^t} \right)^2 \|\mathbb{E}_{\mathbf{g} \sim \mathcal{N}(0, \mathbf{I}_{U^\perp})} [\xi_{\mathbf{g}}(\theta_t) \mathbf{g}]\|^2 \\ &\quad + \frac{2}{p^t} \langle \nabla F(\theta_t), \mathbb{E}_{\mathbf{g} \sim \mathcal{N}(0, \mathbf{I}_U)} [\xi_{\mathbf{g}}(\theta_t) \mathbf{g}] \rangle + \frac{2}{1-p^t} \langle \nabla F(\theta_t), \mathbb{E}_{\mathbf{g} \sim \mathcal{N}(0, \mathbf{I}_{U^\perp})} [\xi_{\mathbf{g}}(\theta_t) \mathbf{g}] \rangle + \\ &\quad + \frac{2}{p^t(1-p^t)} \langle \mathbb{E}_{\mathbf{g} \sim \mathcal{N}(0, \mathbf{I}_U)} [\xi_{\mathbf{g}}(\theta_t) \mathbf{g}], \mathbb{E}_{\mathbf{g} \sim \mathcal{N}(0, \mathbf{I}_{U^\perp})} [\xi_{\mathbf{g}}(\theta_t) \mathbf{g}] \rangle\end{aligned}$$

And therefore by Cauchy Schwartz:

$$\left| \|\mathbb{E}_{\mathbf{g} \sim \hat{\mathcal{P}}} [z_1]\|^2 - \|\nabla F(\theta_t)\|^2 \right| \leq \frac{1}{(p^t)^2} \frac{\sigma^4 \tau^2 d_{\text{active}}^4}{4} + \frac{1}{(1-p^t)^2} \frac{\sigma^4 \tau^2 d_\perp^4}{4} + \frac{2}{p^t} L \frac{\sigma^2 \tau d_{\text{active}}^2}{4} + \frac{2}{1-p^t} L \frac{\sigma^2 \tau d_\perp^2}{4} + \frac{2}{p^t(1-p^t)} \frac{\sigma^4 \tau^2 d_{\text{active}}^2 d_\perp^2}{16}$$

As desired.  $\square$

**Bounding the variance of  $z_{ES}$  and  $z_1$ .**

**Theorem 6.5.** *If  $F$  satisfies Assumption 1 and 2, the variance of the ES estimator satisfies:*

$$|\text{Var}_{ES} - (d+1)\|\nabla F(\theta_t)\|^2| \leq 105\tau^2\sigma^4d^4 + 6\tau\sigma^2Ld^2 + 15d^3\sigma^2L\tau + 105\tau^2\sigma^4d^4$$

$$\text{If } \sigma < \frac{1}{35} \sqrt{\frac{\epsilon \min(p^t, 1-p^t)}{\tau d^3 \max(L, 1)}}:$$

$$|\text{Var}_{ES} - (d+1)\|\nabla F(\theta_t)\|^2| \leq \epsilon$$

*Proof.* The second moment of the ES estimator satisfies:

$$\begin{aligned} \mathbb{E}_{\mathbf{g} \sim \mathcal{N}(0, \mathbf{I})} [z_{ES}^\top z_{ES}] &= \mathbb{E}_{\mathbf{g} \sim \mathcal{N}(0, \mathbf{I})} \left[ \frac{(F(\theta_t + \sigma \mathbf{g}) - F(\theta_t - \sigma \mathbf{g}))^2}{2^2 \sigma^2} \mathbf{g}^\top \mathbf{g} \right] \\ &= \mathbb{E}_{\mathbf{g} \sim \mathcal{N}(0, \mathbf{I})} \left[ (\mathbf{g}^\top \nabla F(\theta_t) + \xi_{\mathbf{g}}(\theta_t))^2 \mathbf{g}^\top \mathbf{g} \right] \\ &= \mathbb{E}_{\mathbf{g} \sim \mathcal{N}(0, \mathbf{I})} \left[ \nabla F(\theta_t)^\top \mathbf{g} \mathbf{g}^\top \mathbf{g} \mathbf{g}^\top \nabla F(\theta_t) + 2 \nabla F(\theta_t)^\top \mathbf{g} \mathbf{g}^\top \mathbf{g} \xi_{\mathbf{g}}(\theta_t) + \xi_{\mathbf{g}}(\theta_t)^2 \mathbf{g}^\top \mathbf{g} \right] \\ &= (d+2)\|\nabla F(\theta_t)\|^2 + 2\mathbb{E}_{\mathbf{g} \sim \mathcal{N}(0, \mathbf{I})} [\nabla F(\theta_t)^\top \mathbf{g} \mathbf{g}^\top \mathbf{g} \xi_{\mathbf{g}}(\theta_t)] + \mathbb{E}_{\mathbf{g} \sim \mathcal{N}(0, \mathbf{I})} [\xi_{\mathbf{g}}(\theta_t)^2 \mathbf{g}^\top \mathbf{g}] \end{aligned}$$

Under Assumption 1 and 2, the following bound for the second and third terms of the last equality holds:

$$|\mathbb{E}_{\mathbf{g} \sim \mathcal{N}(0, \mathbf{I})} [\nabla F(\theta_t)^\top \mathbf{g} \mathbf{g}^\top \mathbf{g} \xi_{\mathbf{g}}(\theta_t)]| \leq \mathbb{E}_{\mathbf{g} \sim \mathcal{N}(0, \mathbf{I})} [\|\nabla F(\theta_t)\| \|\mathbf{g}\|^6] \leq 15d^3\sigma^2L\tau$$

And:

$$|\mathbb{E}_{\mathbf{g} \sim \mathcal{N}(0, \mathbf{I})} [\xi_{\mathbf{g}}(\theta_t)^2 \mathbf{g}^\top \mathbf{g}]| \leq \tau^2\sigma^4 \mathbb{E}_{\mathbf{g} \sim \mathcal{N}(0, \mathbf{I})} [\|\mathbf{g}\|^8] \leq 105\tau^2\sigma^4d^4$$

Therefore:

$$\text{Var}_{ES} = \underbrace{\mathbb{E}_{\mathbf{g} \sim \mathcal{N}(0, \mathbf{I})} \left[ \frac{(F(\theta_t + \sigma \mathbf{g}) - F(\theta_t - \sigma \mathbf{g}))^2}{2^2 \sigma^2} \mathbf{g}^\top \mathbf{g} \right]}_{\diamond} - \underbrace{\left\| \mathbb{E}_{\mathbf{g} \sim \mathcal{N}(0, \mathbf{I})} \left[ \frac{F(\theta_t + \sigma \mathbf{g}) - F(\theta_t - \sigma \mathbf{g})}{2\sigma} \mathbf{g} \right] \right\|^2}_{\spadesuit}$$

After coalescing the bounds derived in the preceding section, we can obtain the following bound on the term  $\diamond$ :

$$|\diamond - (d+2)\|\nabla F(\theta_t)\|^2| \leq 15d^3\sigma^2L\tau + 105\tau^2\sigma^4d^4$$

Notice that by virtue of 10, the following bound on term  $\spadesuit$  of the previous equation holds:

$$|\spadesuit - \|\nabla F(\theta_t)\|^2| \leq 105\tau^2\sigma^4d^4 + 6\tau\sigma^2Ld^2$$

Combining these two inequalities the result follows. □

A similar theorem holds for  $z_1$ .

**Theorem 6.6.**

$$\left| \text{Var}_{\hat{P}} - \left( \frac{d_{\text{active}} + 2}{p^t} \|\mathbf{U}^\top \nabla F(\theta_t)\|^2 + \frac{d_\perp + 2}{1 - p^t} \|(\mathbf{U}^\perp)^\top F(\theta_t)\|^2 - \|\nabla F(\theta_t)\|^2 \right) \right| \leq \frac{1}{p^t} (15d_{\text{active}}^3 \sigma^2 L \tau + 105\tau^2 \sigma^4 d_{\text{active}}^4) + \frac{1}{1 - p^t} (15d_\perp^3 \sigma^2 L \tau + 105\tau^2 \sigma^4 d_\perp^4) + \frac{1}{(p^t)^2} \frac{\sigma^4 \tau^2 d_{\text{active}}^4}{4} + \frac{1}{(1 - p^t)^2} \frac{\sigma^4 \tau^2 d_\perp^4}{4} + \frac{2}{p^t} L \frac{\sigma^2 \tau d_{\text{active}}^2}{4} + \frac{2}{1 - p^t} L \frac{\sigma^2 \tau d_\perp^2}{4} + \frac{2}{p^t(1 - p^t)} \frac{\sigma^4 \tau^2 d_{\text{active}}^2 d_\perp^2}{16}$$

If  $\sigma < \frac{1}{35} \sqrt{\frac{\epsilon \min(p^t, 1 - p^t)}{\tau d^3 \max(L, 1)}}$ :

$$\left| \text{Var}_{\hat{P}} - \left( \frac{d_{\text{active}} + 2}{p^t} \|\mathbf{U}^\top \nabla F(\theta_t)\|^2 + \frac{d_\perp + 2}{1 - p^t} \|(\mathbf{U}^\perp)^\top F(\theta_t)\|^2 - \|\nabla F(\theta_t)\|^2 \right) \right| \leq \epsilon$$

*Proof.* The second moment of  $z_1$  satisfies:

$$\mathbb{E}_{\mathbf{g} \sim \hat{P}} [z_1^\top z_1] = \frac{1}{p^t} \mathbb{E}_{\mathbf{g} \sim \mathcal{N}(0, \mathbf{I}_U)} \left[ \frac{(F(\theta_t + \sigma \mathbf{g}) - F(\theta_t - \sigma \mathbf{g}))^2}{2^2 \sigma^2} \mathbf{g}^\top \mathbf{g} \right] + \frac{1}{1 - p^t} \mathbb{E}_{\mathbf{g} \sim \mathcal{N}(0, \mathbf{I}_{U^\perp})} \left[ \frac{(F(\theta_t + \sigma \mathbf{g}) - F(\theta_t - \sigma \mathbf{g}))^2}{2^2 \sigma^2} \mathbf{g}^\top \mathbf{g} \right]$$

Notice that:

$$\text{Var}_{\hat{P}} = \underbrace{\mathbb{E}_{\mathbf{g} \sim \hat{P}} \left[ \frac{(F(\theta_t + \sigma \mathbf{g}) - F(\theta_t - \sigma \mathbf{g}))^2}{2^2 \sigma^2} \mathbf{g}^\top \mathbf{C}_1^{-2} \mathbf{g} \right]}_{\diamond} - \underbrace{\left\| \mathbb{E}_{\mathbf{g} \sim \hat{P}} \left[ \frac{F(\theta_t + \sigma \mathbf{g}) - F(\theta_t - \sigma \mathbf{g})}{2\sigma} \mathbf{C}_1^{-1} \mathbf{g} \right] \right\|^2}_{\spadesuit}$$

By a similar argument as that in the previous theorem, we conclude:

$$\left| \diamond - \frac{d_{\text{active}} + 2}{p^t} \|\mathbf{U}^\top \nabla F(\theta_t)\|^2 - \frac{(d_{V^\perp} + 2)}{1 - p^t} \|(\mathbf{U}^\perp)^\top \nabla F(\theta_t)\|^2 \right| \leq \frac{1}{p^t} (15d_{\text{active}}^3 \sigma^2 L \tau + 105\tau^2 \sigma^4 d_{\text{active}}^4) + \frac{1}{1 - p^t} (15d_\perp^3 \sigma^2 L \tau + 105\tau^2 \sigma^4 d_\perp^4)$$

By Theorem 6.4:

$$|\spadesuit - \|\nabla F(\theta_t)\|^2| \leq \frac{1}{(p^t)^2} \frac{\sigma^4 \tau^2 d_{\text{active}}^4}{4} + \frac{1}{(1 - p^t)^2} \frac{\sigma^4 \tau^2 d_\perp^4}{4} + \frac{2}{p^t} L \frac{\sigma^2 \tau d_{\text{active}}^2}{4} + \frac{2}{1 - p^t} L \frac{\sigma^2 \tau d_\perp^2}{4} + \frac{2}{p^t(1 - p^t)} \frac{\sigma^4 \tau^2 d_{\text{active}}^2 d_\perp^2}{16}$$

□

## 6.2. Variance reduction via non isotropic sampling

As a consequence of the results of the previous sections we obtain the following Theorem:

**Theorem 6.7.** Let  $\epsilon > 0$ . If  $\sigma < \frac{1}{35} \sqrt{\frac{\epsilon \min(p^t, 1-p^t)}{\tau d^3 \max(L, 1)}}$  then:

$$\left\| \mathbb{E}_{\mathbf{g} \sim \mathcal{N}(0, \mathbf{I})} [z_{ES}] - \nabla F(\theta_t) \right\| \leq \epsilon \quad (12)$$

$$\left\| \mathbb{E}_{\mathbf{g} \sim \hat{\mathcal{P}}} [z_1] - \nabla F(\theta_t) \right\| \leq \epsilon \quad (13)$$

and

$$|\text{Var}_{ES} - (d+1)\|\nabla F(\theta_t)\|^2| \leq \epsilon \quad (14)$$

$$\left| \text{Var}_{\hat{\mathcal{P}}} - \left( \frac{d_{\text{active}} + 2}{p^t} \|\mathbf{U}^\top \nabla F(\theta_t)\|^2 + \frac{d_\perp + 2}{1-p^t} \|(\mathbf{U}^\perp)^\top \nabla F(\theta_t)\|^2 - \|\nabla F(\theta_t)\|^2 \right) \right| \leq \epsilon \quad (15)$$

We say that in this case:

$$\text{Var}_{\hat{\mathcal{P}}} \approx \underbrace{\left( \frac{d_{\text{active}} + 2}{p^t} \|\mathbf{U}^\top \nabla F(\theta_t)\|^2 + \frac{d_\perp + 2}{1-p^t} \|(\mathbf{U}^\perp)^\top \nabla F(\theta_t)\|^2 - \|\nabla F(\theta_t)\|^2 \right)}_{\text{Var}_{\hat{\mathcal{P}}}^M}$$

and  $\text{Var}_{ES} \approx (d+1)\|\nabla F(\theta_t)\|^2$ . We refer to  $\text{Var}_{\hat{\mathcal{P}}}^M$  as the "main component" of the variance  $\text{Var}_{\hat{\mathcal{P}}}$ . Similarly we define  $\text{Var}_{ES}^M = (d+1)\|\nabla F(\theta_t)\|^2$  and use the same name, "main component" of the variance  $\text{Var}_{ES}^M$ .

The optimal  $p^t$ , that which minimizes  $\text{Var}_{\hat{\mathcal{P}}}^M$  equals:

$$(p^t)^* = \frac{\|(\nabla F(\theta_t))_{\text{active}}\| \sqrt{d_{\text{active}} + 2}}{\|(\nabla F(\theta_t))_{\text{active}}\| \sqrt{d_{\text{active}} + 2} + \|(\nabla F(\theta_t))_\perp\| \sqrt{d_\perp + 2}}$$

*Proof.* Roughly the same argument as above yields the desired result.  $\square$

**Lemma 6.8.** The optimal variance  $\text{Var}_{\hat{\mathcal{P}}^*}^M$  corresponding to  $(p^t)^*$  equals:

$$\left[ \|(\nabla F(\theta_t))_{\text{active}}\| \sqrt{d_{\text{active}} + 2} + \|(\nabla F(\theta_t))_\perp\| \sqrt{d_\perp + 2} \right]^2 - \|\nabla F(\theta_t)\|^2 \quad (16)$$

*Proof.* The statement follows directly from substituting the expression for  $(p^t)^*$  into the variance formula.  $\square$

**Theorem 6.9.**  $\text{Var}_{\hat{\mathcal{P}}^*}^M \leq \text{Var}_{ES}^M$  if

$$|\sqrt{d_{\text{active}} + 2} \|(\nabla F(\theta_t))_\perp\| - \sqrt{d_\perp + 2} \|(\nabla F(\theta_t))_{\text{active}}\|| \geq \sqrt{2} \|\nabla F(\theta_t)\| \quad (17)$$

*Proof.* By definition,  $\text{Var}_{\hat{\mathcal{P}}^*}^M < \text{Var}_{ES}^M$  if:

$$\left( \|(\nabla F(\theta_t))_{\text{active}}\| \sqrt{d_{\text{active}} + 2} + \|(\nabla F(\theta_t))_\perp\| \sqrt{d_\perp + 2} \right)^2 < \|\nabla F(\theta_t)\|^2 (d+2) \quad (18)$$

Let  $a_1 = \sqrt{d_{\text{active}} + 2}$ ,  $a_2 = \sqrt{d_\perp + 2}$ ,  $b_1 = \|(\nabla F(\theta_t))_{\text{active}}\|$ ,  $b_2 = \|(\nabla F(\theta_t))_\perp\|$ ,  $a = \sqrt{d+2}$  and  $b = \|\nabla F(\theta_t)\|$ .

The following relationships hold:  $b_1^2 + b_2^2 = b^2$  and  $a_1^2 + a_2^2 - 2 = a^2$ . The bound we want to prove in Equation 18 reduces to finding conditions under which:

$$(a_1 b_1 + a_2 b_2)^2 \leq (b_1^2 + b_2^2)(a_1^2 + a_2^2 - 2)$$

Which holds iff:

$$2b_1^2 + 2b_2^2 \leq a_2^2 b_1^2 + a_1^2 b_2^2 - 2a_1 a_2 b_1 b_2$$

The later holds iff:

$$|a_1 b_2 - a_2 b_1| \geq \sqrt{2}b$$

Which holds iff:

$$\left| \sqrt{d_{\text{active}} + 2} \|(\nabla F(x_t))_{\perp}\| - \sqrt{d_{\perp} + 2} \|(\nabla F(x_t))_{\text{active}}\| \right| \geq \sqrt{2} \|\nabla F(x_t)\|$$

□

The inequality is strict for example when  $\|(\nabla F(x_t))_{\perp}\| = 0$  and  $d_{\perp} \geq 1$ .

This in turn implies that:

**Theorem 6.10.** *If  $\sigma$  is as small as defined at the beginning of the section, we denote by  $\text{Var}_{(\hat{P})^*}$  as the variance of the gradient estimator under mechanism 1 for the optimal (for  $\text{Var}_{\hat{P}}^M$ ) probability  $(p^t)^*$ :*

$$\text{Var}_{\hat{P}^*} \leq \text{Var}_{ES} + \epsilon$$

### 6.3. Estimating the sensing ratio $r$ .

Recall the definitions  $s_{\mathbf{U}^{\text{act}}} = \|\mathbf{U}^{\top} \nabla F(\theta_t)\|^2$  and  $s_{\mathbf{U}^{\perp}} = \|(\mathbf{U}^{\perp})^{\top} \nabla F(\theta_t)\|^2$ .

Since  $\left| \frac{F(\theta_t + \sigma \mathbf{g}) - F(\theta_t - \sigma \mathbf{g})}{2\sigma} - \mathbf{g}^{\top} \nabla F(\theta_t) \right| \leq \xi_{\mathbf{g}}(\theta_t)$ , when  $\mathbf{g} \sim \hat{P}$ , we recognize two cases. If  $\mathbf{g} \sim \mathcal{N}(0, \mathbf{I}_{\mathbf{U}})$  the distribution of  $\frac{F(\theta_t + \sigma \mathbf{g}) - F(\theta_t - \sigma \mathbf{g})}{2\sigma} \approx N(0, \|\mathbf{U}^{\top} \nabla F(\theta_t)\|^2)$ . Analogously when  $\mathbf{g} \sim \mathcal{N}(0, \mathbf{I}_{\mathbf{U}^{\perp}})$  the distribution of  $\frac{F(\theta_t + \sigma \mathbf{g}) - F(\theta_t - \sigma \mathbf{g})}{2\sigma} \approx N(0, \|(\mathbf{U}^{\perp})^{\top} \nabla F(\theta_t)\|^2)$ .

**Theorem 6.11.** *Let  $0 < s < C$  and let  $\mathbf{g}_i \sim \mathcal{N}(0, \mathbf{I}_{\mathcal{L}_{\text{active}}^{\text{ES}}})$  for  $i = 1, \dots, s$  and  $\mathbf{g}_i \sim \mathcal{N}(0, \mathbf{I}_{\mathcal{L}_{\text{active}}^{\text{ES}, \perp}})$  for  $i = s + 1, \dots, C$ .*

*Let  $\hat{s}_{\mathbf{U}^{\text{ort}}} := \frac{1}{s} \sum_{j=1}^s \left( \frac{F(\theta_t + \sigma \mathbf{g}_j) - F(\theta_t - \sigma \mathbf{g}_j)}{2\sigma} \right)^2$ ,  $\hat{s}_{\mathbf{U}^{\perp}} := \frac{1}{C-s} \sum_{j=1}^{C-s} \left( \frac{F(\theta_t + \sigma \mathbf{g}_j) - F(\theta_t - \sigma \mathbf{g}_j)}{2\sigma} \right)^2$  and let  $\hat{r} = \sqrt{\frac{\hat{s}_{\mathbf{U}^{\text{ort}}}}{\hat{s}_{\mathbf{U}^{\perp}}}}$ . Given  $u, \epsilon > 0$  and  $\delta \in (\epsilon, 1)$ , the following holds.*

1. *If  $C = 2s$  for  $s \geq \frac{16}{u^2} \log\left(\frac{8}{\delta}\right)$  and under the mechanism from Algorithm 2 or*
2. *If  $\{\mathbf{g}_i\}_{i=1}^C$  are samples generated under  $\hat{P}$ ,  $\min(p^t, 1 - p^t) > u$  and  $C \geq \max\left(\frac{8}{(p^t - u)u^2}, \frac{8}{(1 - p^t - u)u^2}, \frac{2p^t + 2u/3}{u^2}\right) \log\left(\frac{12}{\delta}\right)$ ,*

*then with probability at least  $1 - \delta$ :*

$$\sqrt{\frac{s_{\mathbf{U}^{\text{ort}}}(1-u) - \frac{2\epsilon}{\delta}}{s_{\mathbf{U}^{\perp}}(1+u) + \frac{2\epsilon}{\delta}}} \leq \hat{r} \leq \sqrt{\frac{s_{\mathbf{U}^{\text{act}}}(1+u) + \frac{2\epsilon}{\delta}}{s_{\mathbf{U}^{\perp}}(1-u) - \frac{2\epsilon}{\delta}}}.$$

*Proof.* First observe we introduce some notation.

$$\xi_{\mathbf{g}}^{(2)}(\theta_t) = \left( \frac{F(\theta_t + \sigma \mathbf{g}) - F(\theta_t - \sigma \mathbf{g})}{2\sigma} \right)^2 - (\mathbf{g}^{\top} \nabla F(\theta_t))^2$$

Observe that:

$$\begin{aligned} \xi_{\mathbf{g}}^{(2)}(\theta_t) &= \left| \left( \frac{F(\theta_t + \sigma \mathbf{g}) - F(\theta_t - \sigma \mathbf{g})}{2\sigma} \right)^2 - (\mathbf{g}^{\top} \nabla F(\theta_t))^2 \right| \\ &\leq \xi_{\mathbf{g}}(\theta_t)^2 + 2 |\mathbf{g}^{\top} \nabla F(\theta_t) \xi_{\mathbf{g}}(\theta_t)| \\ &\leq \sigma^4 \tau^2 \|\mathbf{g}\|^6 + 2\sigma^2 \tau L \|\mathbf{g}\|^4 \end{aligned}$$

Let  $\hat{s}_V = \hat{s}_V^0 + \frac{1}{s} \sum_{j=1}^s \xi_{\mathbf{g}_j}(\theta_t)$  and  $\hat{s}_{V^\perp} = \hat{s}_{V^\perp}^0 + \frac{1}{C-s} \sum_{j=1}^{C-s} \xi_{\mathbf{g}_j}(\theta_t)$ . Where  $s_{\mathbf{U}^{\text{act}}}^0 = \frac{1}{s} \sum_{j=1}^s (\nabla F(\theta_t)^\top \mathbf{g}_j)^2$  and  $s_{\mathbf{U}^\perp}^0 = \frac{1}{C-s} \sum_{j=1}^{C-s} (\nabla F(\theta_t)^\top \mathbf{g}_j)^2$ .

Notice that  $\nabla F(\theta_t)^\top \mathbf{g}$  is distributed as a Gaussian Random variable (with variance depending on the support of the covariance of  $\mathbf{g}$ ).

By concentration of squared gaussian random variables:

$$\begin{aligned} \mathbb{P} [|\hat{s}_V^0 - s_{\mathbf{U}^{\text{act}}}| \geq us_{\mathbf{U}^{\text{act}}}] &\leq 2 \exp\left(-\frac{su^2}{8}\right) \\ \mathbb{P} [|\hat{s}_{V^\perp}^0 - s_{\mathbf{U}^\perp}| \geq us_{\mathbf{U}^\perp}] &\leq 2 \exp\left(-\frac{(k-s)u^2}{8}\right) \end{aligned}$$

Consequently, with probability  $1 - 2 \exp\left(-\frac{su^2}{8}\right) - 2 \exp\left(-\frac{(k-s)u^2}{8}\right)$ , it holds that:

$$\frac{s_{\mathbf{U}^{\text{act}}}}{s_{\mathbf{U}^\perp}} \left(\frac{1+u}{1-u}\right) \geq \frac{\hat{s}_V^0}{\hat{s}_{V^\perp}^0} \geq \frac{s_{\mathbf{U}^{\text{act}}}}{s_{\mathbf{U}^\perp}} \left(\frac{1-u}{1+u}\right)$$

Notice that by Markov's inequality:

$$\mathbb{P} \left( \xi_{\mathbf{g}}(\theta_t) \geq \frac{2\epsilon}{\delta} \right) \leq \delta \frac{\mathbb{E} [\sigma^4 \tau^2 \|\mathbf{g}\|^6 + 2\sigma^2 \tau L \|\mathbf{g}\|^4]}{2\epsilon} \leq \frac{\delta}{2} \quad (19)$$

Since  $\sigma < \frac{1}{35} \sqrt{\frac{\epsilon \min(p^t, 1-p^t)}{\tau d^3 \max(L, 1)}}$ ,  $\mathbb{E} [\sigma^4 \tau^2 \|\mathbf{g}\|^6 + 2\sigma^2 \tau L \|\mathbf{g}\|^4] \leq \epsilon$ .

Regardless if  $\mathbf{g}$  was sampled from  $\mathcal{N}(0, \mathbf{I})$ ,  $\mathcal{N}(0, \mathbf{I}_{\mathbf{U}})$  or  $\mathcal{N}(0, \mathbf{I}_{\mathbf{U}^\perp})$ .

### Case 1.

By definition,  $C = 2s$ , and therefore  $C - s = C/2$  and therefore:

$$\begin{aligned} \mathbb{P} [|\hat{s}_V^0 - s_{\mathbf{U}^{\text{act}}}| \geq us_{\mathbf{U}^{\text{act}}}] &\leq 2 \exp\left(-\frac{Cu^2}{16}\right) \\ \mathbb{P} [|\hat{s}_{V^\perp}^0 - s_{\mathbf{U}^\perp}| \geq us_{\mathbf{U}^\perp}] &\leq 2 \exp\left(-\frac{Cu^2}{16}\right) \end{aligned}$$

We require that:

$$\begin{aligned} 2 \exp\left(-\frac{Cu^2}{16}\right) &\leq \delta/4 \\ 2 \exp\left(-\frac{Cu^2}{16}\right) &\leq \delta/4 \end{aligned}$$

### Case 2.

In fact, by concentration results on Bernoulli variables, given  $\alpha > 0$ ,  $|s - kp^t| \leq k\alpha$  and  $|(k-s) - (1-p^t)k| \leq k\alpha$  with probability at least  $1 - \exp\left(-\frac{k\alpha^2}{2p^t}\right) - \exp\left(-\frac{k\alpha^2}{2p^t+2\alpha/3}\right)$ .

Let  $\alpha = u$ . Conditioning on the events that  $|s - kp^t| \leq uk$  and  $|(k-s) - (1-p^t)k| \leq uk$ . We seek to ensure that:

$$\begin{aligned}
 2 \exp\left(-\frac{(p^t - u)ku^2}{8}\right) &\leq \delta/6 \\
 2 \exp\left(-\frac{(1 - p^t - u)ku^2}{8}\right) &\leq \delta/6 \\
 \exp\left(-\frac{ku^2}{2p^t}\right) &\leq \delta/6 \\
 \exp\left(-\frac{ku^2}{2p^t + 2u/3}\right) &\leq \delta/6
 \end{aligned}$$

**Case 1 and 2** The following inequalities hold:

$$\frac{s_{\mathbf{U}^{\text{act}}}(1 - u) - \frac{2\epsilon}{\delta}}{s_{\mathbf{U}^\perp}(1 + u) + \frac{2\epsilon}{\delta}} \leq \frac{\hat{s}_V^0 - \frac{2\epsilon}{\delta}}{\hat{s}_{V^\perp}^0 + \frac{2\epsilon}{\delta}} \leq \frac{\hat{s}_V}{\hat{s}_{V^\perp}} \leq \frac{\hat{s}_V^0 + \frac{2\epsilon}{\delta}}{\hat{s}_{V^\perp}^0 - \frac{2\epsilon}{\delta}} \leq \frac{s_{\mathbf{U}^{\text{act}}}(1 + u) + \frac{2\epsilon}{\delta}}{s_{\mathbf{U}^\perp}(1 - u) - \frac{2\epsilon}{\delta}}$$

The union bound yields the desired result. And therefore the result follows.  $\square$

#### 6.4. Adaptive Mirror Descent for variance reduction.

Let  $\mathbf{p}^l = \begin{pmatrix} p^l \\ 1 - p^l \end{pmatrix}$ . The main component  $\Gamma$  of the variance of  $\widehat{\nabla}_{\text{MC}, k=1}^{\text{AT, asebo}} F_\sigma(\theta)$  as a function of  $\mathbf{p}^l$  equals (Lemma 3.3) :

$$\Gamma = \ell(\mathbf{p}^l) = \frac{d_{\text{active}} + 2}{\mathbf{p}^l(1)} s_{\mathbf{U}^{\text{act}}} + \frac{d_\perp + 2}{\mathbf{p}^l(2)} s_{\mathbf{U}^\perp} - \|\nabla F(\theta)\|^2.$$

In order to avoid the gradients to explode in norm, we parametrise  $\mathbf{p}^l$  as follows:

$$\mathbf{p}^l = (1 - 2\beta)\mathbf{q}^l + \begin{pmatrix} \beta \\ \beta \end{pmatrix}$$

For  $\mathbf{q}^l \in \Delta_2$  and  $\beta \in (0, 1)$ , the boundary probability bias.

Notice that  $\Gamma$  is a convex function of  $\mathbf{p}$  and also a convex function of  $\mathbf{q}$ . With a slight abuse of notation we denote  $\ell(\mathbf{q}^l)$  as the loss parametrized by  $\mathbf{q}^l$  (which satisfies  $\ell(\mathbf{q}^l) = \ell(\mathbf{p}^l)$ ).

The gradient  $\nabla_{\mathbf{q}^l} \ell(\mathbf{q}^l)$  equals:

$$\nabla_{\mathbf{q}^l} \ell(\mathbf{q}^l) = (1 - 2\beta) \begin{pmatrix} -\frac{d_{\text{active}} + 2}{((1 - 2\beta)\mathbf{q}^l(1) + \beta)^2} s_{\mathbf{U}^{\text{act}}} \\ -\frac{d_\perp + 2}{((1 - 2\beta)\mathbf{q}^l(2) + \beta)^2} s_{\mathbf{U}^\perp} \end{pmatrix},$$

And can be approximated (at the cost of some bias) using function evaluations.

**Lemma 6.12.** *The gradient  $\nabla_{\mathbf{q}^l} \ell(\mathbf{q}^l)$  satisfies:*

$$\left\| \nabla_{\mathbf{q}^l} \ell(\mathbf{q}^l) - \mathbb{E} \left[ (1 - 2\beta) \begin{pmatrix} -\frac{a_l(d_{\text{active}} + 2)}{((1 - 2\beta)\mathbf{p}^l(1) + \beta)^3} v_l^2 \\ -\frac{(1 - a_l)(d_\perp + 2)}{((1 - 2\beta)\mathbf{p}^l(2) + \beta)^3} v_l^2 \end{pmatrix} \right] \right\| \leq \frac{\epsilon(d + 2)}{(\min(\mathbf{p}^l(1), \mathbf{p}^l(2)))^3} \leq \frac{\epsilon(d + 2)}{\beta^3},$$

where  $v_l = \frac{1}{2\sigma} (F(\theta + \mathbf{g}_l) - F(\theta - \mathbf{g}_l))$ .

*Proof.* We start with some notation borrowed from the previous section:

$$\xi_{\mathbf{g}_l}^{(2)}(\theta) = \underbrace{\left( \frac{F(\theta + \sigma\mathbf{g}_l) - F(\theta - \sigma\mathbf{g}_l)}{2\sigma} \right)^2}_{v_l^2} - (\mathbf{g}_l^\top \nabla F(\theta_t))^2$$

Observe that:

$$\begin{aligned} |\xi_{\mathbf{g}_l}^{(2)}(\theta)| &= \left| \left( \frac{F(\theta + \sigma \mathbf{g}_l) - F(\theta - \sigma \mathbf{g}_l)}{2\sigma} \right)^2 - (\mathbf{g}_l^\top \nabla F(\theta))^2 \right| \\ &\leq \xi_{\mathbf{g}_l}(\theta)^2 + 2 |\mathbf{g}_l^\top \nabla F(\theta) \xi_{\mathbf{g}_l}(\theta)| \\ &\leq \sigma^4 \tau^2 \|\mathbf{g}_l\|^6 + 2\sigma^2 \tau L \|\mathbf{g}_l\|^4 \end{aligned}$$

Since  $\sigma < \frac{1}{35} \sqrt{\frac{\epsilon \min(p^l, 1-p^l)}{\tau d^3 \max(L, 1)}}$ :

$$\mathbb{E} \left[ |\xi_{\mathbf{g}_l}^{(2)}(\theta)| \right] \leq \epsilon$$

The result follows. □

Let  $p^l = (1 - 2\beta)q^l + \beta$  be the probability that we choose to sample from the subspace  $\mathcal{L}_{\text{active}}^{\text{ES}}$  and  $1 - p^l$  the probability that we choose to sample from  $\mathcal{L}_{\text{active}}^{\text{ES}, \perp}$ . Let  $a_l$  be a Bernoulli random variable  $a_l \in \{0, 1\}$  with  $\mathbb{E} \left[ \begin{pmatrix} a_l \\ 1-a_l \end{pmatrix} \right] = \mathbf{p}^l$ . Define the stochastic gradient (with respect to  $\mathbf{q}^l$ ):

$$\mathbf{e}_l = (1 - 2\beta) \begin{bmatrix} \left( -\frac{a_l(d_{\text{active}}+2)}{p_l^3} \right) \\ \left( -\frac{(1-a_l)(d_{\perp}+2)}{(1-p_l)^3} \right) \end{bmatrix} v_l^2$$

By definition this random vector (conditioned on the choice of  $\mathbf{p}^l$ ) satisfies:

$$\|\mathbb{E}[\mathbf{e}_l] - \nabla_{\mathbf{q}^l} \ell(\mathbf{q}^l)\| \leq \frac{\epsilon(d+2)}{(\min(\mathbf{p}^l(1), \mathbf{p}^l(2)))^3} \leq \frac{\epsilon(d+2)}{\beta^3},$$

If  $\epsilon$  is chosen small enough, the bias can be driven to be arbitrarily small.

#### 6.4.1. MIRROR DESCENT

We treat this problem as that of minimizing the loss  $\ell$  over the two dimensional simplex and resort to adapt a version of Mirror descent for it. As opposed the case of projected gradient descent, mirror descent performs updates that are adapted to the geometry of the simplex, ensuring the iterates always belong to the simplex and no projection step is necessary. The mirror descent updates are:

$$\begin{aligned} \mathbf{q}_l(1) &= \frac{\mathbf{q}_{l-1}(1) \exp(-\alpha \mathbf{e}_l(1))}{\mathbf{q}_{l-1}(1) \exp(-\alpha \mathbf{e}_l(1)) + (\mathbf{q}_{l-1}(2)) \exp(-\alpha \mathbf{e}_l(2))} \\ \mathbf{q}_l(2) &= \frac{\mathbf{q}_{l-1}(2) \exp(-\alpha \mathbf{e}_l(2))}{\mathbf{q}_{l-1}(1) \exp(-\alpha \mathbf{e}_l(1)) + (\mathbf{q}_{l-1}(2)) \exp(-\alpha \mathbf{e}_l(2))} \end{aligned}$$

For a step size parameter  $\alpha$ .

#### 6.5. Regret guarantees

Using the notation in <https://www.stat.berkeley.edu/~bartlett/courses/2014fall-cs294stat260/lectures/mirror-descent-notes.pdf>, In this case let  $R(\mathbf{q}) = \mathbf{q}(1) \log(\mathbf{q}(1)) + \mathbf{q}(2) \log(\mathbf{q}(2)) - \mathbf{q}(1) - \mathbf{q}(2)$  and therefore:

$$\nabla R(\mathbf{q}) = \begin{pmatrix} \log(\mathbf{q}(1)) \\ \log(\mathbf{q}(2)) \end{pmatrix} \quad (20)$$

The Fenchel conjugate of  $R$  equals:

$$R^*(\mathbf{q}) = e^{\mathbf{q}(1)} + e^{\mathbf{q}(2)} \quad (21)$$

And therefore the gradient of the Fenchel conjugate equals:

$$\nabla R^*(\mathbf{q}) = \begin{pmatrix} \exp(\mathbf{q}(1)) \\ \exp(\mathbf{q}(2)) \end{pmatrix} \quad (22)$$

And:

$$D_R(\mathbf{q}_1, \mathbf{q}_2) = \mathbf{q}_1(1) \log \left( \frac{\mathbf{q}_1(1)}{\mathbf{q}_2(1)} \right) + \mathbf{q}_1(2) \log \left( \frac{\mathbf{q}_1(2)}{\mathbf{q}_2(2)} \right) + \mathbf{q}_2(1) - \mathbf{q}_1(1) + \mathbf{q}_2(2) - \mathbf{q}_1(2) \quad (23)$$

Recall the update behind Mirror descent takes the form (stepsize  $\alpha$ ):

1. Play  $(\frac{a_l}{1-a_l})$  such that  $\mathbb{E}[(\frac{a_l}{1-a_l})] = \mathbf{p}^l$ .
2. Let  $w_{l+1} = \nabla R^*(\nabla R(\mathbf{p}^l) - \alpha \mathbf{e}_l)$
3. Let  $\mathbf{p}^{l+1} = \arg \min_{\mathbf{p} \in \Delta_2} D_R(\mathbf{p}, w_{l+1})$

Recall the general definition of Bregman divergence:

$$D_\Psi(u, v) = \Psi(u) - \Psi(v) - \langle \nabla \Psi(v), u - v \rangle \quad (24)$$

The following regret guarantee holds for Mirror descent (see <https://www.stat.berkeley.edu/~bartlett/courses/2014fall-cs294stat260/lectures/mirror-descent-notes.pdf>):

**Theorem 6.13.** *If at time  $l$  a convex loss function  $f_l$  is revealed to the player and the player performs the mirror descent step using  $\nabla f_l$  as a proxy linear function, with actions (from the mirror descent step)  $a_l$  at time  $l$ , for any  $a$  in the intersection of all of  $f_l$ 's domains, the following regret bound holds:*

$$\sum_{l=1}^C (f_l(a_l) - f_l(a)) \leq \sum_{l=1}^C \nabla f_l(a_l)^\top (a_l - a) \quad (25)$$

$$\leq \frac{1}{\alpha} \left( R(a) - R(a_1) + \sum_{l=1}^C D_{R^*}(\nabla R(a_l) - \alpha \nabla f_l(a_l), \nabla R(a_l)) \right) \quad (26)$$

Also remember that if  $R^*$  is  $\theta$ -smooth with respect to some norm  $\|\cdot\|$ , we can upper bound  $D_{R^*}$ . The former ( $R^*$  being  $\theta$ -smooth) holds if  $R$  is  $\frac{1}{\theta}$ -strongly convex with respect to the dual norm  $\|\cdot\|_*$ . When  $R$  equals the entropy, this is 1-strongly convex with respect to the  $L_1$  norm and hence  $R^*$  is 1-strongly smooth with respect to the  $L_\infty$  norm:

$$D_{R^*}(a, b) \leq \frac{\|a - b\|_\infty^2}{2} \quad (27)$$

In our case, let  $f_l(\mathbf{q}) = \mathbf{e}_l^\top \mathbf{q}$ . Using the upper bound previously described for  $D_{R^*}$ . For any  $\mathbf{q} \in \Delta_2$ :

$$\sum_{l=1}^C f_l(\mathbf{q}^l) - f_l(\mathbf{q}) \leq \frac{1}{\alpha} \left( R(\mathbf{q}) - R(\mathbf{q}^1) + \alpha^2 \sum_{l=1}^C \frac{\|\nabla f_l(\mathbf{q}_l)\|_\infty^2}{2} \right)$$

Taking expectations, since  $\left| \mathbb{E}[f_l(\mathbf{q}) | \mathbf{q}_l] - \nabla_{\mathbf{q}^l} \ell(\mathbf{q}^l) \mathbf{q} \right| \leq \frac{\epsilon(d+2)}{\beta^3}$  we obtain the following result:

$$\left( \sum_{l=1}^C \nabla_{\mathbf{q}^l}^\top \ell(\mathbf{q}^l) (\mathbf{q}^l - \mathbf{q}) \right) - C \frac{2\epsilon(d+2)}{\beta^3} \leq \frac{1}{\alpha} \left( R(\mathbf{q}) - \mathbb{E}[R(\mathbf{q}^l)] + \alpha^2 \sum_{l=1}^C \frac{\mathbb{E}[\|\mathbf{e}_l\|_\infty^2]}{2} \right)$$

Now we bound the Right Hand side of the expression above. Notice that  $R(\mathbf{q}) \leq 2$  and  $R(\mathbf{q}_1) \geq 0$ . We can also bound the expectation  $\mathbb{E}[\|\mathbf{e}_l\|_\infty^2]$ .

**Lemma 6.14.**  $|\mathbb{E}[\|\mathbf{e}_l\|^2] - \|\nabla_{\mathbf{q}^l} \ell(\mathbf{q}^l)\|^2| \leq \frac{\epsilon(d+1)}{\beta^3}$

*Proof.* A similar calculation as in Lemma 6.12 yields the desired result.  $\square$

Since:

$$\mathbb{E}[\|\mathbf{e}_l\|_\infty^2] \leq \mathbb{E}[\|\mathbf{e}_l\|^2] \quad (28)$$

And  $\|\nabla_{\mathbf{q}^l} \ell(\mathbf{q}^l)\|^2 \leq \frac{1}{\beta^4} ((d_{\text{active}} + 2)^2 s_{\mathbf{U}_{\text{ort}}}^2 + (d_\perp + 2)^2 s_{\mathbf{U}_\perp}^2)$ .

We obtain the following bound:

$$\left( \sum_{l=1}^C \nabla_{\mathbf{q}^l}^\top \ell(\mathbf{q}^l) (\mathbf{q}^l - \mathbf{q}) \right) - C \frac{2\epsilon(d+2)}{\beta^3} \leq \frac{2}{\alpha} + \frac{\alpha C}{2\beta^4} ((d_{\text{active}} + 2)^2 s_{\mathbf{U}_{\text{ort}}}^2 + (d_\perp + 2)^2 s_{\mathbf{U}_\perp}^2) + \frac{\alpha C \epsilon (d+1)}{\beta^3}$$

The following theorem follows:

**Theorem 6.15.** If  $\alpha = \frac{2\beta^2}{\sqrt{C} \sqrt{(d_{\text{active}} + 2)^2 s_{\mathbf{U}_{\text{ort}}}^2 + (d_\perp + 2)^2 s_{\mathbf{U}_\perp}^2}}$  and  $\epsilon = \frac{\beta^3}{2C(d+1)}$ , for any  $\mathbf{q} \in \Delta_2$ :

$$\left( \sum_{l=1}^C \nabla_{\mathbf{q}^l}^\top \ell(\mathbf{q}^l) (\mathbf{q}^l - \mathbf{q}) \right) \leq \frac{\sqrt{C} \sqrt{(d_{\text{active}} + 2)^2 s_{\mathbf{U}_{\text{ort}}}^2 + (d_\perp + 2)^2 s_{\mathbf{U}_\perp}^2}}{\beta^2} + 1$$

*Proof.* Plugging in this value of  $\alpha$ :

$$\begin{aligned} \left( \sum_{l=1}^C \nabla_{\mathbf{q}^l}^\top \ell(\mathbf{q}^l) (\mathbf{q}^l - \mathbf{q}) \right) &\leq \frac{\sqrt{C} \sqrt{(d_{\text{active}} + 2)^2 s_{\mathbf{U}_{\text{ort}}}^2 + (d_\perp + 2)^2 s_{\mathbf{U}_\perp}^2}}{\beta^2} \\ &+ \left( 1 + \frac{2\beta^2}{\sqrt{C} \sqrt{(d_{\text{active}} + 2)^2 s_{\mathbf{U}_{\text{ort}}}^2 + (d_\perp + 2)^2 s_{\mathbf{U}_\perp}^2}} \right) \frac{C\epsilon(d+1)}{\beta^3} \end{aligned}$$

By setting  $\epsilon = \frac{\beta^3}{2C(d+1)}$  the result follows. Assuming  $C$  is large enough so that  $\alpha < 1$ .  $\square$

Since  $\ell(\mathbf{q})$  is a convex function of  $\mathbf{q}$  for all  $l$  and  $\mathbf{q} \in \Delta_2$ :

$$\ell(\mathbf{q}^l) - \ell(\mathbf{q}) \leq \nabla_{\mathbf{q}^l}^\top \ell(\mathbf{q}^l) (\mathbf{q}^l - \mathbf{q})$$

Which in turn implies the main result of this section:

**Theorem 6.16.** If  $\alpha = \frac{2\beta^2}{\sqrt{C} \sqrt{(d_{\text{active}} + 2)^2 s_{\mathbf{U}_{\text{ort}}}^2 + (d_\perp + 2)^2 s_{\mathbf{U}_\perp}^2}}$  and  $\epsilon = \frac{\beta^3}{2C(d+1)}$ , for any  $\mathbf{q} \in \Delta_2$ :

$$\mathbb{E} \left[ \sum_{l=1}^C \ell(\mathbf{q}^l) - \ell(\mathbf{q}) \right] \leq \frac{\sqrt{C} \sqrt{(d_{\text{active}} + 2)^2 s_{\mathbf{U}_{\text{ort}}}^2 + (d_\perp + 2)^2 s_{\mathbf{U}_\perp}^2}}{\beta^2} + 1$$

This is equivalent to the result stated in the main paper.

## 7. Additional Experimental Results

### 7.1. Reinforcement Learning

Here we present three additional environments, LQR, Hopper and full experiment details for Reacher. All experimental details are as in Section 4.

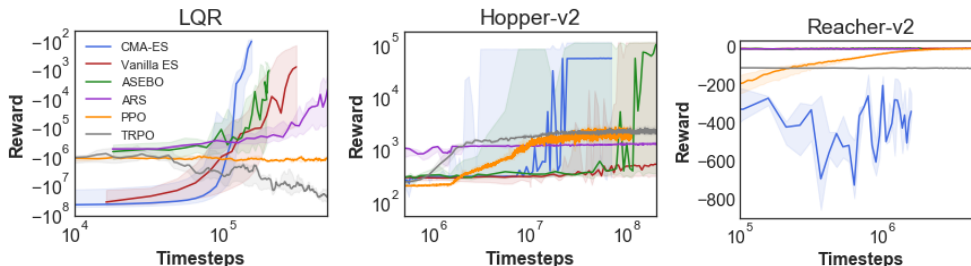


Figure 5. Comparison of different blackbox optimization algorithms on OpenAI Gym tasks and LQR task from (Mania et al., 2018). For environments in plots (a)(b), we show the  $y$ -axis on a log-scale to enable easier comparison amongst algorithms. Plot (c) shows the full Reacher experiment with all baseline algorithms, where we can see that CMA-ES/PPO/TRPO are greatly outperformed by the other methods which we show in the main paper.

As shown in Fig. 5 (a) and (b), for both LQR and Hopper, CMA-ES performs best, with ASEBO second. In Fig. 5 (c), we show the full experiment of Reacher-v2 with evaluations of all baseline algorithms. We find that CMA-ES/PPO/TRPO are greatly outperformed by the other methods which we show in the main paper. In particular, CMA-ES/TRPO barely make progress while PPO learns steadily yet slowly. From the plot we cannot visually distinguish the learning curves of ASEBO, Vanilla ES and ARS since they all achieve fairly fast learning. In the main paper, we have presented a *zoomed-in* plot of the Reacher-v2 experiment, where we show their differences with more granularity.

Below, we discuss in more details our observations from Fig. 5 in the Appendix and Fig. 3 in the main paper.

**State Normalization.** State-of-the-art policy optimization baselines such as PPO/TRPO (Dhariwal et al., 2017) and the original ARS (Mania et al., 2018) apply state normalization as part of the implementation. In particular, the algorithms maintain a component-wise running average of mean  $\bar{s}$  and standard deviation vector  $\sigma(s)$  of the state. When at given state  $s_t$ , the algorithm computes the normalized state  $\tilde{s}_t = \frac{s_t - \bar{s}}{\sigma(s)}$  before inputting to the policy network to compute actions  $a_t = \pi(\tilde{s}_t)$ . For PPO/TRPO, since the optimization is based on back-propagation of neural networks, properly scaling the inputs  $s_t \rightarrow \tilde{s}_t$  is critical for the performance. In all experiments, we remove state normalization mechanism from the implementation to test the robustness of various blackbox optimization algorithms. Notice that as reported by (Mania et al., 2018), state normalization was not needed in ARS to learn good policies for RL tasks under consideration in this paper. As a result, we observe that PPO/TRPO underperform other ES algorithms for most tasks.

**LQR.** The LQR environment was proposed in (Mania et al., 2018) to test the stability of algorithms. Though LQR has relatively low-dimensional observation/action space ( $|\mathcal{S}| = |\mathcal{A}| = 3$ ), the environment parameters are determined such that the dynamics can easily diverge (and lead to low rewards). For policy optimization algorithms, LQR has been shown to be difficult despite its simple linear dynamics, since the learning algorithms need to account for a long horizon. ES-type methods are well suited for this task since the gradient estimates are derived from the total episodic returns. We observe that among ES-type methods, ASEBO comes second to CMA-ES.

### 7.2. Nevergrad blackbox functions

Here we present the results for three additional functions from the Nevergrad library: cigar, sphere and sphere4. In all three cases, ASEBO performs better than Vanilla ES for the base function, and outperforms both Vanilla ES and CMA-ES for the manifold version.

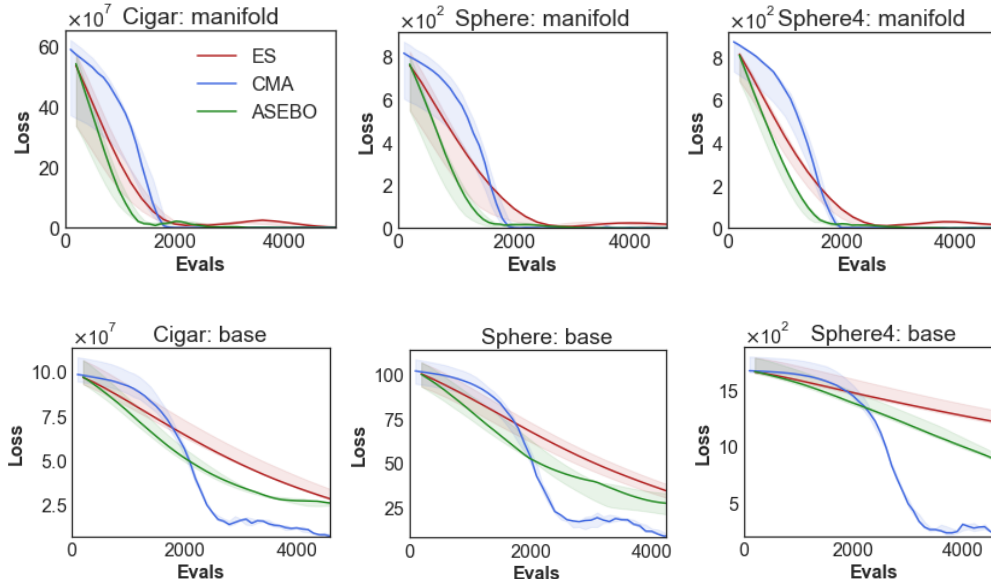


Figure 6. Comparison of different blackbox optimization algorithms on functions from Nevergrad library (Teytaud & Rapin, 2018). All curves are median-curves obtained from  $k = 5$  seeds and with inter-quartile ranges presented as shadowed regions.

## 8. Additional Implementation Details

In this section we present additional details on our experimental results, for both the RL tasks and Nevergrad functions.

### 8.1. Reinforcement Learning Experiment Details

We provide additional details regarding the RL experiments below.

**Benchmark Environments.** Benchmark environments are from OpenAI gym (Brockman et al., 2016). These environments have variable sizes of observation space and action space: Swimmer-v2  $|\mathcal{S}| = 8$ ,  $|\mathcal{A}| = 2$ ; Hopper-v2  $|\mathcal{S}| = 11$ ,  $|\mathcal{A}| = 3$ ; HalfCheetah-v2  $|\mathcal{S}| = 17$ ,  $|\mathcal{A}| = 6$ ; Walker2d-v2  $|\mathcal{S}| = 17$ ,  $|\mathcal{A}| = 6$ ; Reacher-v2  $|\mathcal{S}| = 11$ ,  $|\mathcal{A}| = 2$ . The LQR environment is based on (Mania et al., 2018) with  $|\mathcal{S}| = 3$ ,  $|\mathcal{A}| = 3$ . All environments have a natural termination condition specified in the simulation environment. For LQR, there is no termination condition but the episodic length is  $T = 300$ .

**Policy Architecture.** All baseline algorithms involve training a parameterized policy  $\pi_{\theta}(a|s)$  using sample gradient estimates generated from the environment. The policy architecture is shared across all algorithms: a 2-layer feed-forward neural network with tanh non-linearity and  $h$  hidden units per layer. The input to the network is the state  $s \in \mathcal{S}$ . For all ES-based algorithms (Vanilla ES, CMA-ES, ARS and ASEBO), the output of the network is the action  $a_{\theta}(s) \in \mathcal{A}$ . For policy optimization algorithms (PPO, TRPO), the output of the network is a mean of Gaussian  $\mu_{\theta}(s)$  and we draw actions from a factorized Gaussian distribution  $a \sim \mathcal{N}(\mu_{\theta}(s), \sigma^2 \mathbb{I})$  where we separately parameterize a standard deviation parameter  $\sigma$  shared across dimensions. The sizes of hidden layers where: 4 for LQR, 16 for Swimmer-v2, Hopper-v2 and Reacher-v2, 32 for HalfCheetah-v2 and Walker2d-v2, reflecting the difficulty of each task.

**Optimization.** Our method (ASEBO) and most baselines (Vanilla ES, ARS, CMA-ES and PPO) apply SGD based methods and we apply the Adam optimizer to stabilize the gradients.

#### 8.1.1. BASELINE ALGORITHMS

**Vanilla ES.** Vanilla ES is the simplest evolutionary algorithm applied in RL tasks (Choromanski et al., 2018; Salimans et al., 2017). We apply the antithetic sampling scheme as applied in (Choromanski et al., 2018). Our implementation does not rank the rewards as in (Salimans et al., 2017), and as previously discussed does not include observation normalization.

**CMA-ES.** Covariance Matrix Adaptation Evolution Strategy is a state-of-the-art and popular black box optimization algorithm (Hansen & Ostermeier, 1996). CMA-ES has been applied as a benchmark algorithm for RL tasks (Duan et al., 2016). We use the open source implementation from *pycma* available at <http://github.com/CMA-ES/pycma>. We use the default hyper-parameters in the original code base with the standard deviation parameter  $\sigma = 1.0$ .

**ARS.** Augmented Random Search (Mania et al., 2018) is based on the code released by the original paper. We use the standard deviation  $\sigma = 0.02$  and learning rate  $\eta = 0.01$ . The hyper-parameters are tuned on top of the default hyper-parameters in the original code base. We remove the observation normalization utility in the original code for fair comparison.

**ASEBO.** We propose Adaptive Sample Efficient Blackbox Optimization in this work. Our algorithms have the following hyper-parameters: the covariance decay parameter  $\lambda = 0.995$  (slow decay), proportion of variance of the active (PCA) space  $\epsilon = 0.995$ , standard deviation parameter  $\sigma = 0.02$ . We set the learning rate  $\eta = 0.02$ .

**Trust Region Policy Optimization.** Trust Region Policy Optimization (TRPO) is based on the implementation of OpenAI baseline (Dhariwal et al., 2017). We use the default training hyper-parameters in the code base: we collect  $N = 1024$  samples per batch to compute a policy gradient, with the trust region size parameter  $\epsilon = 0.01$ . We remove the observation normalization utility in the original code for fair comparison.

**Proximal Policy Optimization.** Proximal Policy Optimization (PPO) (Schulman et al., 2017) is also based on the implementation of OpenAI baseline (Dhariwal et al., 2017). We use the default hyper-parameters in the code base: we collect  $N = 2048$  samples per batch to compute policy gradients and set the clipping coefficient  $\epsilon = 0.2$ . The learning rate is set to be  $\alpha = 3 \cdot 10^{-5}$  for all environments. We remove the observation normalization utility in the original code for fair comparison.

## 8.2. Nevergrad Experiment Details

**Function Settings.** We tested the following functions: cigar, ellipsoid, sphere, sphere4 and lunacek. We created two versions of each function:

- base: Where the function directly depends on the higher-dimensional input.
- manifold: Where the function implicitly depends on the manifold of lower intrinsic dimensionality  $d_{\text{int}}$ . This is achieved by evaluating  $F(Ax)$  where  $A$  is an  $d_{\text{int}} \times d$  random Gaussian matrix, and  $d$  is the dimensionality of the input vector  $x = 100$ . We set  $d_{\text{int}} = 0.05 \times d$  for all problems, which is not known by the algorithm in advance.

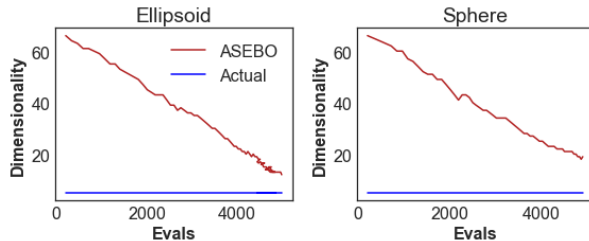


Figure 7. These plots demonstrate ASEBO’s ability to learn the implicit dimensionality of the problem on-the-fly. For the two functions in this figure, we show the dimensionality of the learned active subspace at each iteration for the manifold problem set-up.

**Algorithm Hyper-Parameters.** We use the same hyper-parameters across both versions of all five functions. For ASEBO and VanillaES, we use  $\eta = 0.02$ . For ASEBO we set  $\lambda = 0.3$ . For CMA – ES we use the default parameters from the *pycma* package.

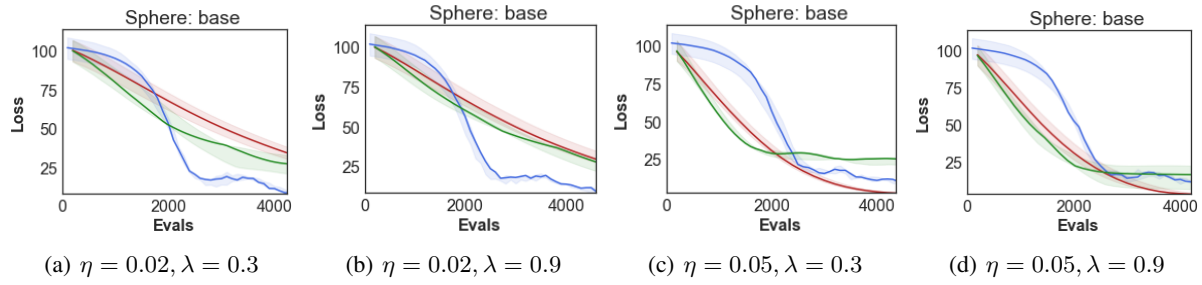


Figure 8. An ablation study examining the impact of changing the learning rate  $\eta$  and decay  $\lambda$  for the sphere function.

As we can see here, increasing  $\eta$  and decreasing  $\lambda$  leads to initially faster learning, at the possible expense of progress later in the optimization.